The Pennsylvania State University

The Graduate School

College of Engineering

SELF-ASSEMBLY AND CHEMICAL PATTERNING ON GERMANIUM(100)

A Thesis in

Engineering Science

by

Jeffrey A. Lawrence

Submitted in Partial Fulfillment
of the Requirements
for the Degree of

Master of Science

August 2010

The thesis of Jeffrey A. Lawrence was reviewed and approved* by the following:

Paul S. Weiss
Distinguished Professor of Chemistry and Physics
Thesis Co-Advisor

Mark W. Horn
Associate Professor of Engineering Science and Mechanics
Thesis Co-Advisor

Tony J. Huang
Associate Professor of Engineering Science and Mechanics

Judith A. Todd
P.B. Breneman Department Head
Head of the Department of Engineering Science and Mechanics

*Signatures are on file in the Graduate School

Abstract

The focus on faster, smaller, and more diverse electronic devices has prompted research into new materials. The search is on for semiconductor substrates with superior electronic capabilities. Germanium has emerged as a semiconductor material capable of producing desired performance. Current methods of thin-film deposition, once intended for applications involving alternative substrates, must be altered to improve upon germanium's inherently unstable surface. This thesis investigates the adolescent mechanism of self-assembly and chemical patterning on Ge(100). Our preliminary research offers insight into applicable techniques for depositing stabilizing and chemically functionalized, patterned adsorbate layers on germanium. It is our belief that the examination of sample preparation will lead to reproducible and cost-efficient techniques for use in industry. This dissertation will address possible candidates for successful monolayer deposition on germanium, and the appearance of and possible solutions to additional limitations.

Germanium suffers from an inherently unstable surface, a result of its native oxide layer. Until this time, instability has limited germanium's capacity for integration into electronic devices. Self-assembled monolayers (SAMs) offer a method for controlling interfacial properties, through formation of highly ordered, single-molecule thick structures on surfaces, transferring their chemical attributes to the interface. Successful deposition of SAMs on germanium can address its intrinsic limitations. Through manipulation of SAM deposition techniques, used primarily for patterning alkanethiols on gold, formation of high-quality monolayers becomes possible, improving the surface stability of germanium.

High-dielectric materials, due to their ability to resist leakage resulting from electron tunneling, are necessary for producing functional components of nanoscale dimensions. These materials may be limited in their ability to interact with relevant substrates, making device fabrication difficult. Chemical patterning techniques exhibit the ability to place an array of species selectively, otherwise limited by surface diffusion, bonding capacity, etc., onto semiconductor surfaces. This dissertation describes the utilization and manipulation of soft lithography methods for successful patterning on germanium.

TABLE OF CONTENTS

List of Figures

List of Abbreviations

Molecules	
AD	1-Adamantanethiol
ALK	Alkanethiol
C2	n-Dithiol
C12	n-Dodecanethiol
C18	n-Octadecanethiol
MUDA	11-Mercaptoundecanoic Acid
OTS	Octadecyltrichlorosilane
PDMS	Polydimethylsiloxane

Patterning Techniques	
CVD	Chemical Vapor Deposition
CVM	Chemical Vapor Machining
DPN	Dip Pen Nanolithography
LPCVD	Low-Pressure Chemical Vapor Deposition
MOCVD	Metal-Organic Chemical Vapor Deposition
PLD	Pulsed-Laser Deposition
PVD	Physical Vapor Deposition
RIE	Reactive Ion Etching
UHV-CVD	Ultrahigh Vacuum Chemical Vapor Deposition

SμCP	Submerged Microcontact Printing
μCP	Microcontact Printing
μCIP	Microcontact Insertion Printing
μDP	Microdisplacement Printing

Characterization Tools

AFM	Atomic Force Microscopy
ATR	Attenuated Total Reflectance
FESEM	Field Emission Scanning Electron Microscopy
IRRAS	Infrared Reflection Absorption Spectroscopy
XPS	X-Ray Photoelectron Spectroscopy

Other Acronyms

BE	Binding Energy
GL	Gaussian-Lorentzian
IRE	Internal Reflection Element
I_{tunnel}	Tunneling Current Set Point
KE	Kinetic Energy
SAM	Self-Assembled Monolayer
UHV	Ultrahigh Vacuum
V_{sample}	Applied Sample Bias

γ_{LV}	Surface Tension at Liquid-Vapor Interface
γ_{SL}	Surface Tension at Solid-Liquid Interface
γ_{SV}	Surface Tension at Solid-Vapor Interface
θ_A	Advancing Contact Angle
θ_C	Equilibrium Contact Angle
θ_R	Receding Contact Angle
θ_S	Sliding Angle
θ_γ	Young's Contact Angle

Acknowledgments

Writing this dissertation has been an interesting experience, to say the least. I would not recommend condensing the thesis writing adventure into a few weeks, but I have discovered it can be done. First, I would like to thank my thesis advisor, Professor Paul S. Weiss. Not only did you afford me the opportunity to explore graduate studies, you continue to offer me every chance at success in the field. I appreciate your understanding demeanor concerning my future plans and your willingness to assist in my endeavors. I would also like to thank you for the indirect supply of motivation necessary for me to start (and quickly finish) this thesis. Professor Mark W. Horn, thank you for taking me on as your advisee. Without your help, I would not have been able to pursue a degree in the engineering field. Additionally, I would like to thank Professor Tony J. Huang for agreeing to serve on my thesis committee. Working predominately within the chemistry department, I knew few engineering science professors, and am glad you agreed to finalize my committee.

I would like to thank the National Science Foundation, the National Science Foundation funded Center for Nanoscale Science, the Army Research Office, the Kavli Foundation, and Penn State's National Nanotechnology Infrastructure Network for their financial support of this work. Additionally, the Penn State University Materials Characterization Laboratory, and especially Dr. Thomas A. Daniel are gratefully acknowledged for data collection and XPS analysis.

The completion of this thesis would not have been possible without the assistance of several other individuals. First, I would like to thank Dr. Steve Stranick. Unsure of my future plans, you encouraged and enabled me to pursue the field of research. My time at N.I.S.T. was informative and enjoyable. Furthermore, without your guidance and recommendations I would have never considered or been able to achieve a graduate degree. Your ability and patience concerning the translation of research concepts into layman's terms has proved incalculable. Additionally, I think I learned just as much on the rides to and from work as I did in the lab. The sports conversations were entertaining, but the amount of information I gained concerning random issues was phenomenal. I think of you not only as a mentor, but as a friend, thank you.

I would also like to extend a big thank you to all of the Weiss group members, past and present. Without your assistance, concerning a number of issues, this would not have been possible. I would especially like to thank Nate Hohman. He guided my research, encouraged me to learn as much as I could, and without his clarification and editing, I doubt this dissertation would have been legible.

Condensing the next few people into one paragraph is almost an injustice. My family. Mom, Dad, Laura, Kevin, and Heather, although I was reluctant to explain, and you would have failed to understand anyway, you always inquired about my progress and offered encouragement. To my extended family (Uncle Bill, Aunt Johnna, Joe, and Nick, consider yourselves included, I appreciate all of your support and maybe someday I will get that PhD), thanks for the prayers and the push to continue through indecision. Rick and Jen, if you lived more than 10 minutes away, there is a good chance that I would be writing this paper in smelly clothing. Hell, I might not be writing it at all as a result of

medical complications related to malnutrition. Furthermore, without the interaction of you and your slightly crazy neighbors (I plan to burn that wood as quickly as possible, so we can look for more, if they even let us see each other), I would have been institutionalized, as a result of my inability to excel socially. To Lilly, Olivia, and Connor; thanks for the comic relief. Without you little ones, boredom would have ensued. I am glad that my graduate work enabled me to watch you guys grow up. Maybe, before you guys get too big, I will use you to find myself a girlfriend, seeing as though your mother has been incapable of doing so. I love you. To the Zeigler crew, Trigger says thanks for the good times around the fire, and the ridiculous hours spent sprinting around the mountain in an attempt to keep up with the "Master." Make sure to pick up any "road closed" signs that you see and we will drop them off on our way to visit Hook and the gang. It is alright to eat the chitlins but stay away from the pepper jack cheese, and if you do either, remember to pack the paper towels. Never forget that every dog has its day, and of course, to all my blood brothers, Voodoo! To all you other fools out there, I call my friends, thanks for using my apartment as a gateway to explore the nightlife of state college. Drinking beers with you guys is just good old fashion fun. Finally, to the big guy upstairs, I am fairly confident that it was you who kept me sane throughout all this. I appreciate it.

Chapter 1

Introduction

1.1 Overview

The self- and directed assembly of molecularly-thick films constitute a powerful tool for use in the areas of nanotechnology, molecular electronics, biochemistry, and bioengineering.[1-8] Extensive research has been conducted to identify quality candidates for controlling interface properties and for the patterning of technologically important substrates. Gold and silicon have emerged as important materials for their stability, scientifically functional characteristics, and molecular compatibility. For this reason, they have been extensively studied and are relatively well understood. The ability to manipulate such substrates and their interfacial properties is key for the advancement of technology as is the incorporation of new materials and novel methods.

Presently, Si remains the most important technological semiconductor for its ability to produce a quality dielectric oxide layer.[6, 7] The SiO_2 oxide layer passivates the surface of silicon and stabilizes the interface between Si and SiO_2.[7] The density of devices per unit area has increased steadily since the development of the integrated circuit, a well-publicized trend known as Moore's law.[9] Recently, the demand for a shift from macroscale to nanoscale electronics has driven a search for new strategies for electronic devices. On such small scales, leakage currents through dielectrics (a result of electron tunneling between features at small length scales) wreak havoc on performance.[7] For this reason, materials with dielectric constants superior to that of SiO_2 are being sought after. With the advent of dielectric films other than SiO_2, semiconductors with better electrical characteristics than those of silicon become preferable.[7] Group IV

semiconductors are the most obvious choice because of their elemental simplicity and their potential for applications in integrated circuits, solar cells, infrared (IR) detectors, and chemical sensors, amongst others.[7]

The intrinsic properties of germanium have made it a potential material for a new generation of fast electronics. Germanium offers excellent intrinsic electrical properties, specifically higher electron and hole mobility than silicon, and a smaller bandgap.[7, 8, 10] Unfortunately, the native germanium oxide is a poor dielectric making it difficult to apply germanium in applications where silicon is poorly suited. Passivation strategies to control the reactivity of silicon are already well-understood, and similar strategies must be developed for germanium if we are to take advantage of its electronic characteristics.[7] The electrical properties of high-dielectric film/substrate interfaces are dependent upon deposition process, deposition parameters, and pre-deposition surface treatments.[8] Engineering and characterization of interfacial properties are critical for assuring optimal electronic performance.[8] With proper experimentation and manipulation, germanium can outperform its predecessors and be used to push the limits of technology.

This dissertation explores the use of self-assembly and chemistry to enable established patterning techniques to extend beyond standard materials and onto the relatively less explored semiconductor substrate Ge(100). I will discuss the surface chemistry of the germanium surface and oxide, and the development of new methods for both controlling that chemistry and extending chemical patterning to germanium surfaces. A number of techniques were used both to develop and to characterize patterned surfaces. For this reason, the remainder of this chapter will provide an introduction to the most important concepts and analysis methods applied in this paper.

A description of self-assembled monolayers, contact angle procedure, chemical patterning and x-ray photoelectron spectroscopy follow.

1.2 Self-Assembled Monolayers

When an organic molecule adsorbs on a metal or metal oxide surface, the free energy of the interface is lowered.[11] Due to the energetically favorable nature of the interaction, metallic surfaces tend to accommodate nearly any organic adsorbate. By carefully controlling the surface and the organic adsorbate, highly ordered structures may be spontaneously generated from a disordered solution, in a process known as self-assembly. These molecules arrange on the surface in accordance to their physical and chemical properties, which can be tailored for this purpose.[12] Self-assembled monolayers (SAMs) offer a method for controlling interfacial properties by forming highly ordered, single-molecule-thick structures on surfaces, transferring its chemical properties to the interface.[12-24] These SAMs are usually organic self-assemblies formed through adsorption of molecules from the gas or liquid phases.[12] The molecules that form SAMs tend to have a strong affinity for the surface, enabling them to displace pre-adsorbed species and to form well-ordered, chemically functional monolayers. Typically, all reactive substrate sites will be occupied within seconds of exposure to the molecular solution. This rapid assembly accounts for the majority of adsorption.[12] After the initial assembly, a re-ordering process occurs on a timescale of hours. During this time, the monolayer tends to maximize adsorbate density, while improving nanoscale order so as to eliminate defects.[12] For a millimolar solution under ambient conditions the initial assembly takes no more than a few minutes and the re-ordering, no more than a

few hours. However, variables in preparation, such as molecular concentration and temperature, can affect the assembly process.[12]

A wide range of substrates, including noble metals, base metals, insulators, alloys, and semiconductors have been used for SAM preparation.[12, 25-32] Substrate materials are found in many forms, including planar surfaces (glass, metal films) and various three-dimensional nanostructures (colloids, nanocrystals, nanorods). The most commonly studied class of SAMs are those formed from the deposition of alkanethiols on Au{111}.[15, 16, 33, 34] The strong affinity of thiols for Au allow it to form exceptionally ordered monolayers with diverse exposed functionality. Gold is a particularly attractive material for a number of spectroscopic and lithographic techniques, as it does not oxidize in air and shows limited catalytic activity.[15]

The stable and well-ordered SAMs of alkanethiols on gold constitute a model system for self-assembly. The interaction between Au{111} and thiol produce strong stabilizing bonds with an enthalpy of ~44 kcal/(per unit) mol.[19] The thiol headgroup interacts with the gold substrate to produce a Au-S bond, and results in loss of the hydrogen atom, presumably in the form of dihydrogen.[12] The exothermic bond formation drives SAM assembly, and enables secondary interactions between adjacent alkyl chains. The methylene groups associated with each alkyl chain contribute an additional ~1 kcal/(per unit) mol of stabilizing van der Waals interactions.[16]

An alkanethiolate SAM is well known to form a hexagonal $(\sqrt{3} \times \sqrt{3})R30°$ unit cell at the Au{111} interface, with a nearest neighbor spacing of ~4.97Å.[18, 19] The interactions between alkyl chains tend to drive a $c(4\times2)$ superlattice structure representative of the methyl groups in relation to the Au surface.[12, 18, 19, 33]

The lateral interactions between these chains drive the ordering of the SAM, and for that reason longer carbon chains show more order as a result of increased van der Waals interactions.[35] In the case of alkanethiols on Au, the molecules exhibit a molecular tilt of ~30° with respect to the surface normal.[34, 36] Figure 1.1 shows the formation of the alkanethiol unit cell and the *c*(4×2) superlattice; as well as the orientation of the alkyl chains in relation to the Au substrate.

The stability and order of SAMs is well documented, but defects do exist. Disruptions in the monolayer can be caused by defects within the substrate and/or inconsistencies in the ordering process of assembly. Substrate defects are natural features of even the most carefully prepared metallic surface, with common features of atomic steps, vacancy islands, and intergrain boundaries.[17] Atomic steps and grain boundaries are intrinsic to crystalline substrates, whereas vacancy islands arise from the chemistry of self-assembly. A typical Au{111} surface exhibits a $(23 \times \sqrt{3})$ reconstruction, and contains a greater density of atoms then the ideal bulk-constructed {111} crystal face.[37] When thiols bond to the surface during the self-assembly process, they release the reconstruction and reduce atomic density of the substrate surface. The healing mechanism of the surface comes in the form of a single atom vacancy, which will typically diffuse until it collides with another vacancy, resulting in the nucleation and growth of a "vacancy island."[37] All three substrate defects result in uneven topography, which is reproduced by the monolayer. Self-assembly defects are present in the form of compositional heterogeneity and domain boundaries. Self-assembly is a thermodynamic process governed by competitive binding.[12] If adsorbates exhibiting strong interactions contact the substrate, they can infuse themselves into an otherwise homogenous

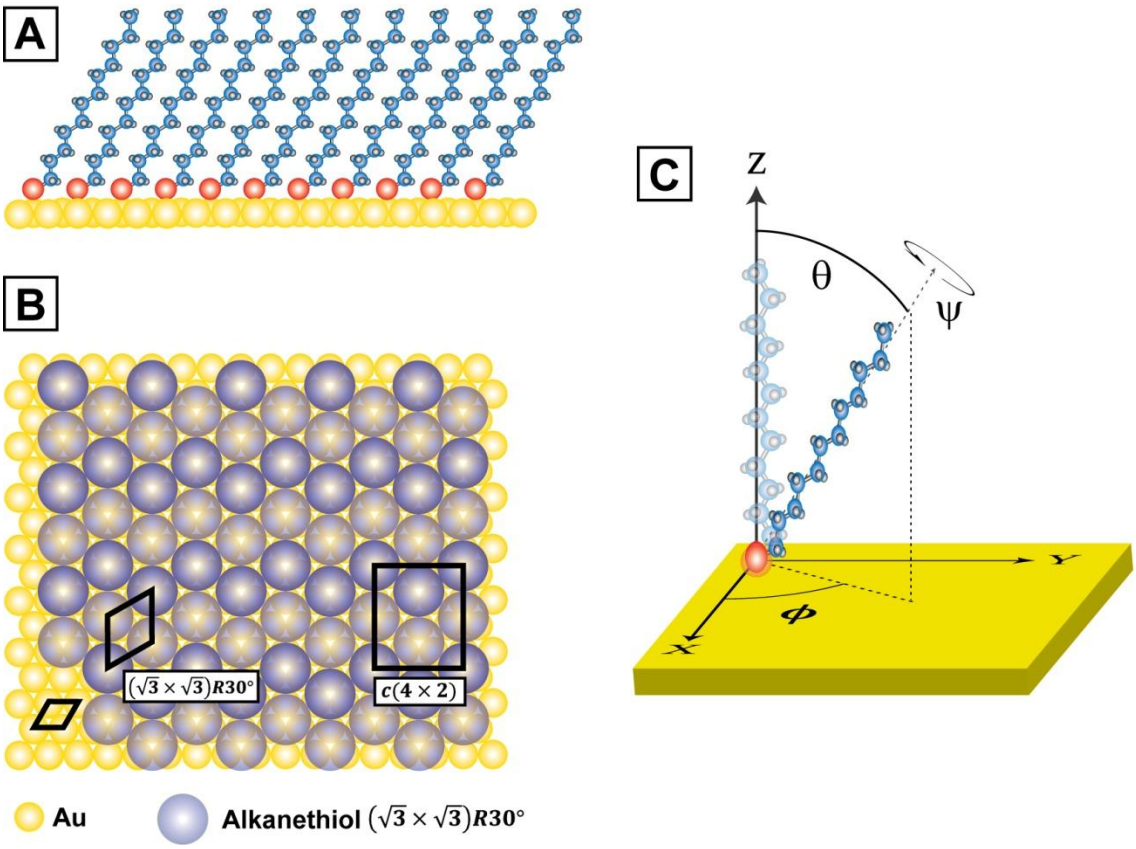

Figure 1.1: Schematic of a *n*-alkanethiol (**ALK**) SAM on a Au{111} substrate. **A.** A side view along the nearest neighbor direction showing the 30° tilt to maximize the van der Waals interactions. **B.** Top down view showing the unit cell of the Au substrate, as well as the $(\sqrt{3} \times \sqrt{3})R30°$ unit cell and the $c(4 \times 2)$ superlattice. Shading highlights the $c(4 \times 2)$ structure. **C.** A single surface-bound all-*trans* **ALK** molecule in which **θ**, **ψ**, and **φ** represent tilt, twist, and azimuth angles of the chain, respectively.[38]

monolayer. A domain boundary is characterized by the intersection of alkyl chains with differing azimuthal tilt angles or offset lattices of attachment. As a result of the chain's dependence on the Au-S packing structure, they may assemble differently, causing multiple orientations on the surface. The red, yellow, and orange arrows in Figure 1.2 depict step edges, vacancy islands, and domain boundaries within a SAM, respectively.

Manipulations of SAMs are far from limited. For example, molecules may be inserted into defects, predominately at step edges and domain boundaries, a technique called insertion.[12] Also, monolayers can be produced such that varying lengths of alkyl chains are codeposited simultaneously on the surface. These mixed monolayers allow the engineering of additional defect sites, many in the form of domain boundaries, where useful chemistry techniques can be applied for the purpose of studying alternative molecules. Self-assembled monolayers have proven to be a useful tool in the development of molecular assemblies and offer a means for controlling the interfacial properties of a metallic surface.

1.3 Contact Angle

The physical characteristics of a liquid droplet on the surface of a solid substrate are dependent upon the chemical and physical interactions at the contact interface. Through careful physical analysis of the droplet, some idea of the interfacial properties can be gained. Contact angle measurement is a straightforward and accurate way of measuring wettability, roughness, interfacial energy, and chemical composition of a surface.[39-41] For this reason, we use the measurement of contact angles as a method for gaining insight into and analysis of surface behavior.

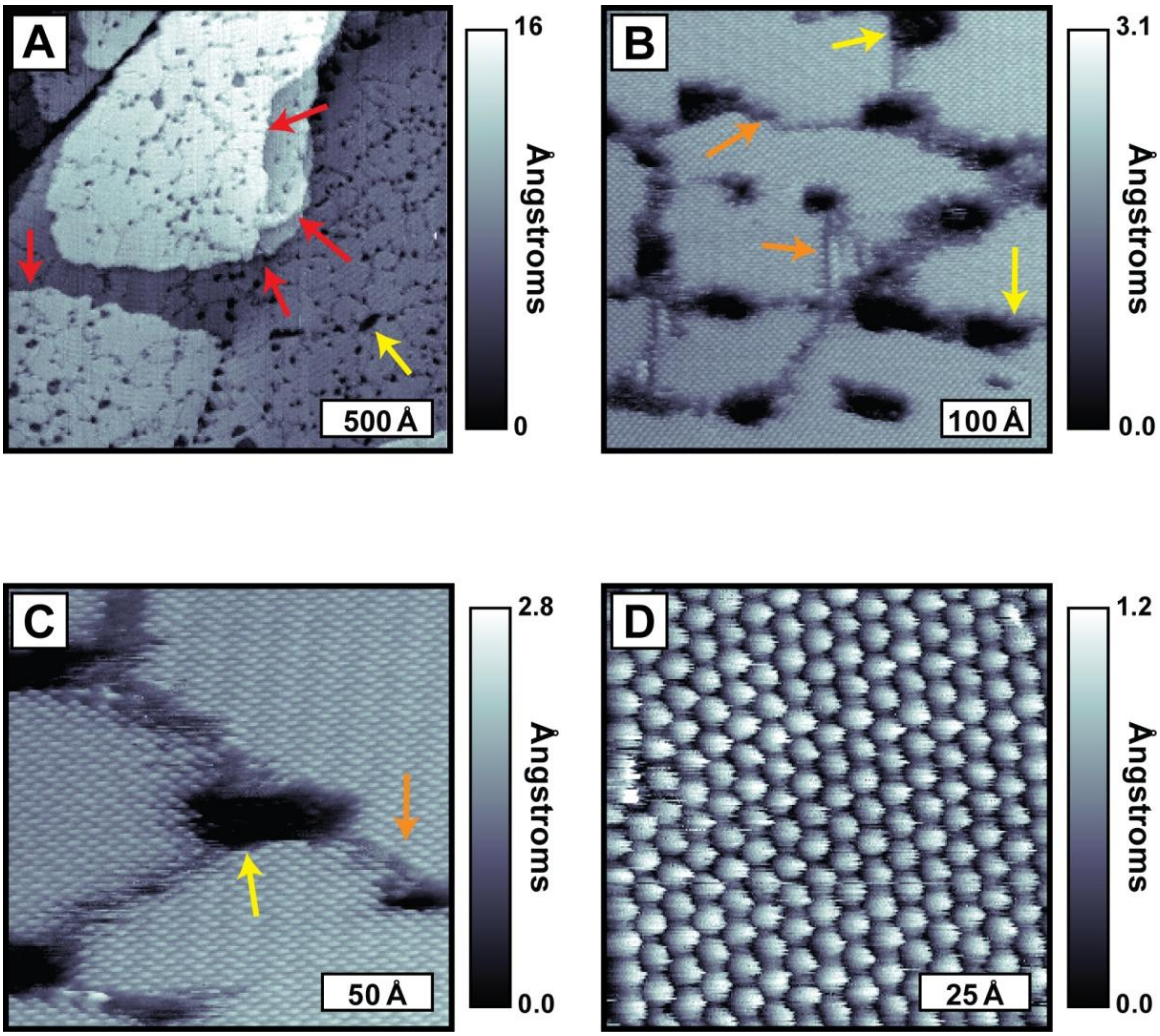

Figure 1.2: Scanning tunneling microscopy images of a **C12** SAM on a Au{111} substrate acquired with a V_{sample} = -1.0 V and a I_{tunnel} = 1.0 pA. The ***red***, ***yellow***, and ***orange*** arrows highlight Au substrate step edges, Au substrate vacancy islands, and molecular domain boundaries, respectively. The circular protrusions correspond to single **C12** molecules.[38]

Three interfaces exist at the point of contact between liquid and solid. The solid-liquid interface, solid-vapor interface, and liquid-vapor interface all express unique interfacial properties. The intersection of the three interfaces will extend along the perimeter of the droplet, and is named the triple or pinning line.[42] The contact angle is measured at a point where the pinning line is reduced to a single point, as is shown in the cross-sectional graph of Figure 1.3, and is defined as "the angle between the solid surface and a tangent drawn to the liquid surface at the point of contact with the solid." [43] The relationship between the three interfaces is expressed by Young's equation:

$$\gamma_{LV}\cos\theta_{\gamma} = \gamma_{SV} - \gamma_{SL}, \tag{1.1}$$

where γ is the surface tension at the interface and θ_{γ} is Young's angle.[41] The subscripts L,V, and S stand for liquid, vapor, and surface, respectively. Surface tension is a physical value representing the amount of work per area necessary to expand a surface.[44] The surface tension for a given material will actively resist expansion. Because every compound exhibits a distinct value for surface tension, the contact angle is a variable dependent upon the interaction between the involved species.

Young's contact angle, also referred to as the equilibrium contact angle, is a product of the interfacial tensions. The equilibrium contact angle occurs when the chemical potential of the three phases is equal and should be singularly constant for a given system. The angle measured by contact angle techniques is rarely consistent with this equilibrium value, as a result of surface impurities.[40] In fact, stable drops may be observed over a range of contact angles. For this reason, contact angles are often defined in terms of two quantities, the advancing angle and receding angle. The advancing angle is defined as the angle associated with an increase in wetted area.[40] Depending on the measurement technique, this could come by way of droplet perimeter expansion, or the

leading edge of a mobile droplet. Likewise, the receding angle is measured for recession in wetted area and can be observed for the lagging edge of moving liquid, or as the drop is shrinking in size. The numerical difference between these two values is known as contact angle hysteresis.[40] Figure 1.4 shows advancing and receding angles as defined for both the tilted wafer method and dynamic sessile drop method.

Hysteresis results from chemical heterogeneity and surface roughness.[45] Surface roughness was first addressed by Robert Wenzel when he suggested that the presence of surface heterogeneity caused the discrepancy between actual surface area and geometrical surface area. Using his modified Young's equation to account for this difference, he proposed that the ratio of actual surface area to geometric surface area be classified as the roughness factor, r.[46] Wenzel's Equation is expressed:

$$\gamma_{LV} \cos\theta_{\gamma} = (\gamma_{SV} - \gamma_{SL})\, r, \tag{1.2}$$

where γ and θ are defined in accordance with Young's equation and r is the roughness factor. This roughness factor accounts for real-world applications where the substrate surface invariably fails to be completely flat. Experimental data have shown that roughening a surface will cause the advancing angle to increase and the receding angle to decrease. In some cases, these results disagree with Wenzel's equation.[40] In either case, a change in angle due to surface roughness is largely a function of surface geometry and is not affected by the interfacial tensions.

The existence of hysteresis suggests the presence of surface roughness and chemical heterogeneity. It is impossible to make conclusions concerning the contributions of either source as they are indistinguishable from the data analysis alone. Only when one source can be completely eliminated can assumptions be made.

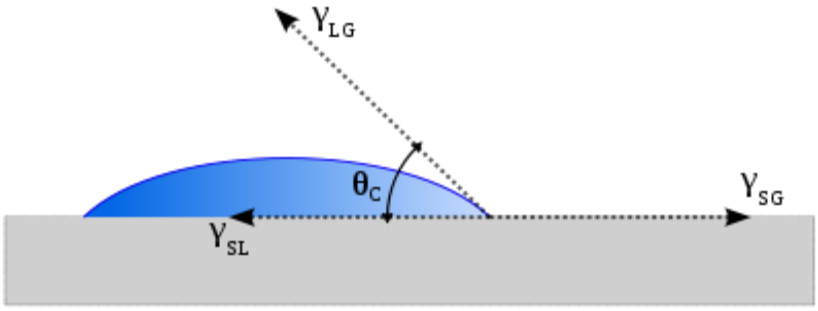

Figure 1.3: Cross-sectional schematic of a liquid droplet on a solid. The arrows represent the location and direction of the surface tension forces associated with the three interfaces. θ_C defines the contact angle.

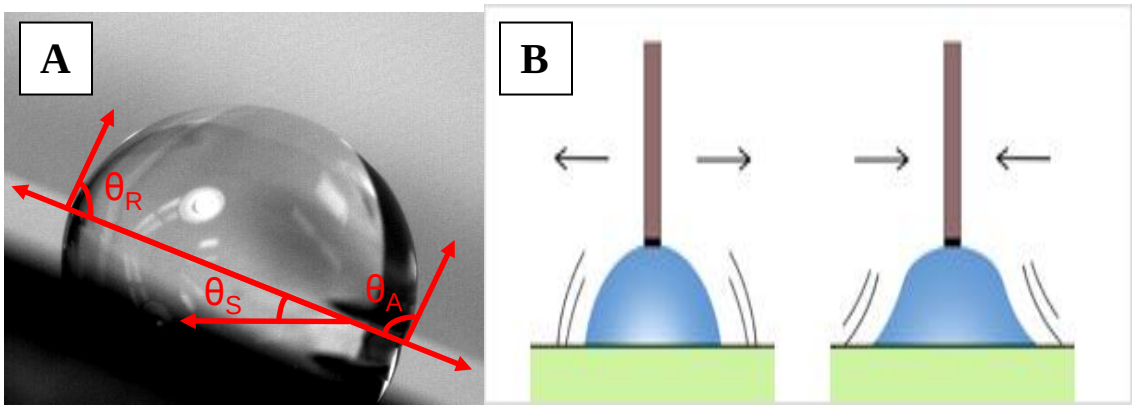

Figure 1.4: **A.** Image representing contact angle measurements by the tilted wafer method. The advancing angle is measured from the leading edge of the drop (down hill side) and is denoted θ_A. The lagging edge produces the receding angle, θ_R. The sliding angle, θ_S, is defined as the degree of tilt directly before sliding motion occurs.[47] **B.** Schematic depicting the addition and reduction of drop size for an increase and decrease in liquid volume, respectively.

For example, if a surface is known to be consistently flat, then the effects of surface roughness are negligible.[45] In this case, the presence of hysteresis is the result of chemical heterogeneity. Furthermore, if it can be determined that hysteresis is caused predominately by chemical impurities, then Young's equation can still be applied to make some statement concerning surface tension.

There are several methods to measure contact angles. Among the most frequently used are the Wilhelmy method, tilted wafer method, and sessile drop method. The Wilhelmy method is a descendent of the Wilhelmy plate method, used to measure a liquid's surface tension. In the Wilhelmy plate method, a plate of known dimensions and buoyancy is exposed to a liquid bath. The plate is suspended from a microbalance and the change in mass after exposure is recorded.[48] Through modification of Young's equation, the advancing and receding angles can be calculated. The tilted wafer method is a dynamic drop method that involves placing a droplet on an angled substrate.[49] The substrate is tilted such that the droplet is on the verge of sliding motion. The leading (or down hill side) of the droplet is measured and recorded as the advancing angle. The trailing edge is measured to gain the receding angle data.[49] For the measurements discussed in this paper, the dynamic sessile drop method was applied. The dynamic sessile drop method utilizes a microsyringe to deposit liquid droplets onto a solid surface. Through addition and subtraction of liquid, the droplet will expand and contract, respectively. The advancing angle is measured while the droplet is in the "filling" mode and the receding angle is recorded during the "emptying" mode.[49] It is generally accepted that an approximate value of the equilibrium angle can be achieved by

averaging the advancing and receding angles. Figure 1.5 defines the contact angle, represented by B.

The evolution of surface tension, and ergo contact angles, associated with a change in chemical composition, is particularly relevant for the work discussed in this dissertation. Here, contact angle measurements were used to measure changes in wettability to track a chemical reaction. We compared the contact angles from a bare, polished Ge(100) wafer to those exposed to various molecular solutions, in hopes of making some statement about the deposition of a monolayer onto the germanium surface. After exposure to dodecanethiol solutions, the contact angle of the surface increased dramatically, consistent with compositional changes in surface chemistry.

1.4 Chemical Patterning

The relevance of chemical patterning is ever increasing. The films produced by patterning techniques are applicable to numerous scientific fields including biological surface science, bio-medicine, and molecular electronics.[1, 3-5, 13, 50-53] There are numerous methods for chemical patterning, many of which fall under the category of soft lithography techniques. Soft lithography is a set of techniques where patterns are transferred to substrates in the absence of energetic beams, by means of soft and flexible materials.[3, 54] Unlike hard lithography and other patterning techniques, soft lithography does not compromise the integrity of the substrate.[3] Soft lithography has exhibited the ability to comply with a large number of adsorbates and substrates. It is utilized in situations where other lithography techniques are incapable of performing, such as patterning applications on curved surfaces and biologically compatible surfaces with

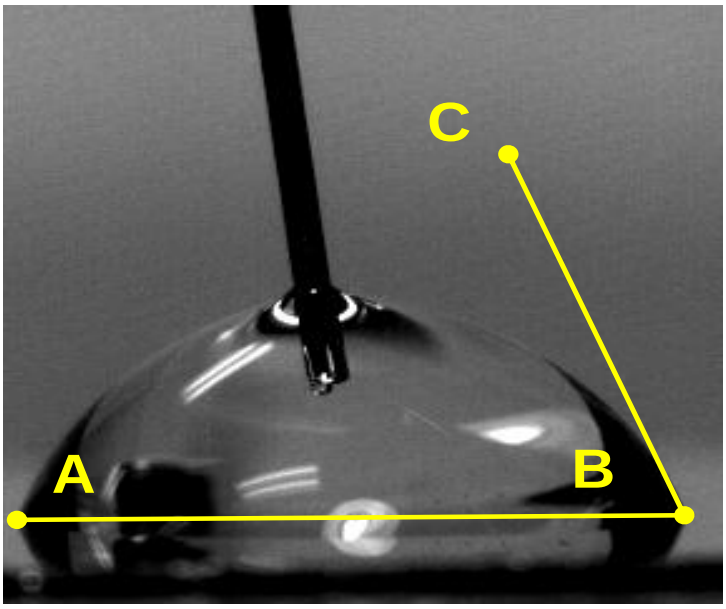

Figure 1.5: Image identifying the measuring parameters of a contact angle. The AB line segment stretches adjacent and parallel to the surface from the point of contact between the drop edge and the surface on the left and right side of the drop. The BC segment begins at the right-most point of the liquid-solid interface and extends tangentially to the drop's surface at that point. The angle of intersection between these two line segments is defined as the contact angle.[47]

feature characteristics on the scale of hundreds of nanometers.[54] Of the many soft lithography techniques, microcontact printing (μCP) emerged as one of the most successful. The typical method for transferring adsorbates to the surface includes a polydimethylsiloxane (**PDMS**) stamp, which has been "inked" with a molecular adsorbate.[3, 50] The elastomeric stamp is designed with surface reliefs that are a mirror image of the desired deposition pattern making selective placement possible.[55] The **PDMS** stamp is soaked in an inking solution, typically a millimolar solution of alkanethiol dissolved in ethanol. After being blow dried, the stamp is pressed mechanically onto the substrate surface. A commonly used substrate of choice is Au{111}, with alkanethiol inks for preparing patterned self-assembled monolayers in contact zones. However, the stamp is capable of patterning onto any thiol-compatible surface. Later in this thesis, a novel method for microcontact printing on Ge(100) will be discussed.

During contact, alkanethiols transfer from the stamp to the substrate and self-assemble according to the relief pattern of the stamp. Figure 1.6 shows a schematic of the stamping process. The resulting SAM is sensitive to the mole fraction of the inking solution, affording some control over the patterning process by varying the thiol concentration.[55-57] In fact, it has been reported in particular cases that chemically patterned SAMs are functionally indistinguishable from SAMs produced by means of solution deposition.[57]

The capabilities of a microcontact-printed surface are numerous. The covalent assembly of the Au/thiol reaction allows for considerable control of the samples

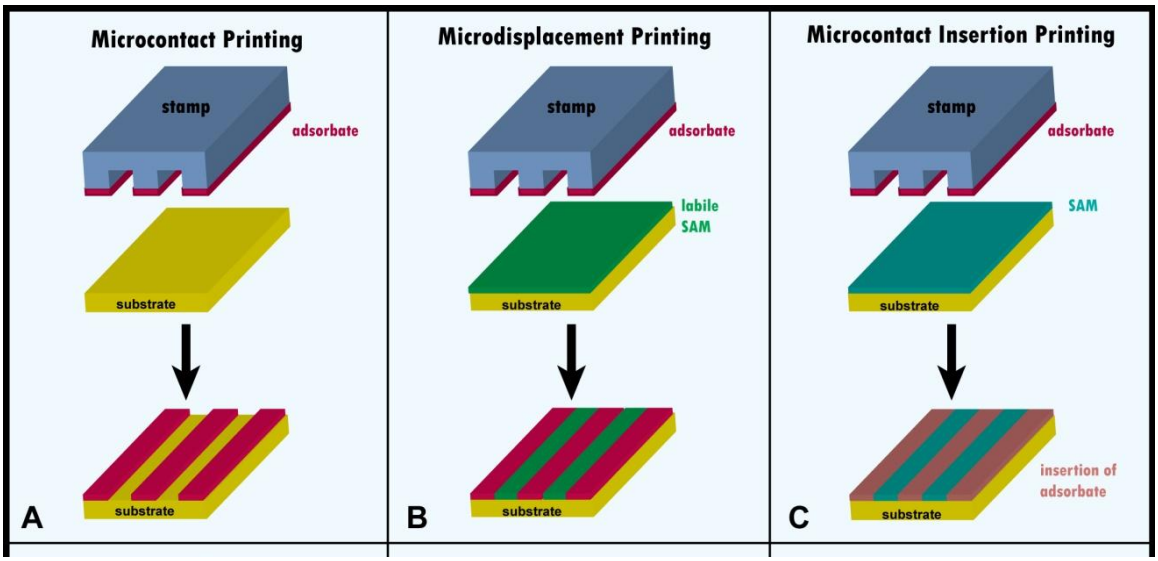

Figure 1.6: Schematic showing basic stamping procedure for soft lithography techniques. In all methods, an etched silicon wafer acts as a master key for producing relief patterns in **PDMS** stamps. **PDMS** is placed in contact with the master to assume its shape. The patterned **PDMS** stamp is peeled from the wafer. It is then soaked in an "inking" solution. **A.** Microcontact printing. The stamp is mechanically pressed upon the Au substrate. After removal, the substrate will have a pattern of SAMs reproducing that of the stamp. **B.** Microdisplacement printing. The inked stamp is mechanically pressed on a Au substrate, pretreated with a labile SAM. The stamp displaces the labile SAM in regions of contact, producing a fully covered surface of labile SAMs, inlaid with inked monolayers. **C**. Microcontact insertion printing. A non-labile SAM is deposited on a Au substrate. Experimental variables control the physical characteristics of the preformed monolayer. Upon contact, the inked stamp deposits inked monolayers into defect sites.[38]

properties. The SAM will actively resist the advancement of etchants and shield its supporting metal substrate from corrosion.[3, 55, 58] The monolayer offers control over surface characteristics including wettability and electrical conductivity.[55, 58] Additional highlights of microcontact printing include cost efficiency, capacity for large printing areas, and the disproportionate relationship between the ease of preparation and the quality of results. Soft lithography does have some negative aspects. Issues with surface diffusion, resolution, and reproducibility have required further development of printing mechanisms.[59]

Microdisplacement printing (μDP) utilizes a substrate with a pre-formed monolayer of 1-adamantanethiolate (**AD**).[59] The use of a pre-formed monolayer is two-fold. First, its presence prevents the lateral diffusion of patterning solutions allowing for a greater variety of applicable molecules. Secondly, **AD** forms a weakly bound SAM on Au and is therefore labile. The labile nature of the molecule allows it to be displaced through competitive adsorption. Therefore, microcontant printing techniques can be applied to replace the labile SAM with a more desirable one.[59] The resulting film is a compilation of **AD** and patterning or "displacing" SAMs.

Another novel printing technique is microcontact insertion printing (μCIP). Like microdisplacement printing, this method utilizes both microcontact techniques and a pre-assembled monolayer.[2] The composition of the patterned SAM can be controlled through manipulation of stamping duration, concentration of molecules, and the quality of the pre-assembled monolayer.[2] Unlike microdisplacement printing, the pre-existing SAM is not labile relative to exchange. Therefore, when the stamp contacts the surface,

the insertion sites are limited by defects. By manipulating the pre-existing film, we gain control over the chemical environment and molecules can be isolated from one another in separated defect sites.[2]

Section 1.5 X-Ray Photoelectron Spectroscopy

Although contact angle measurements are a quality diagnostic for identifying some surface behavior, they do not provide detailed information about the chemistry of the surface. In order to decipher what was occurring on the pre- and post-treated germanium surface, we require a surface-selective and chemically specific analysis technique. X-ray photoelectron spectroscopy (XPS) offers definitive evidence concerning the chemical composition of the surface in question. To aid in the understanding and interpretation of the XPS data present in this dissertation, we will briefly address the principles of this spectroscopic technique.

X-ray photoelectron spectroscopy utilizes incident photons for the excitation and emission of core electrons from surface atoms. Mono-energetic x-rays irradiate a solid surface, and by means of the photoelectric effect, enable surface electrons to escape the bulk in the form of photoelectrons.[60] X-ray photoelectron spectroscopy is surface selective, because photoelectrons in solids are characterized by a small mean free path, and cannot reach the detector if they are generated in the bulk of the material. To improve surface selectivity further, Mg Kα and Al Kα x-rays are typically used for their low penetrating depths in metal (1-10 μm).[60] Although electrons produced deeper then a few tens of Ångstroms below the surface can be emitted, they will incur significant inelastic energy loss. Those electrons produced within tens of Ångstroms of the surface can

escape without energy loss and provide the most useful data.[60] The kinetic energy (KE) of the photoelectron is given by:

$$KE = h\nu - BE - \varphi, \tag{1.3}$$

where hν is the energy of the incident photon, φ is the work function of the spectrometer, and BE is the orbital's binding energy. Binding energy is classified as the difference between the initial and final energy states of the atom after emission. It is also defined as a value proportional to the difference in energy between an electron's orbital and the Fermi level of the solid. Higher orbital electrons dwell closer to the Fermi level and thus require less energy to break existing bonds.

The XPS instrument analyzes the emitted photoelectrons. The raw data translates to a plot of the number or intensity of electrons per energy interval versus kinetic or binding energy. Because every element has characteristic electronic orbitals and a related variety of ionic states, it will thus display a distinctive spectrum of photoelectron emission.[60] Through analysis of a sample's energy signature, the occupying elements can be identified. Furthermore, for a sample of mixed composition, the spectrum will reveal an approximate sum of peaks belonging to the individual elements.[60] Their identities and concentrations can be measured. Conveniently, spectra have already been measured for many of the elements and some basic elemental combinations, simplifying the identification of chemical unknowns. Figure 1.7 depicts an XPS survey spectrum. Note that every peak correlates to a specific binding energy and atomic orbital. Also, note the Au 4d peak(s). As the surface is excited by incident photons the atoms become ionized, and illuminate the spin states of slightly different kinetic energy of the surface atoms.[60]

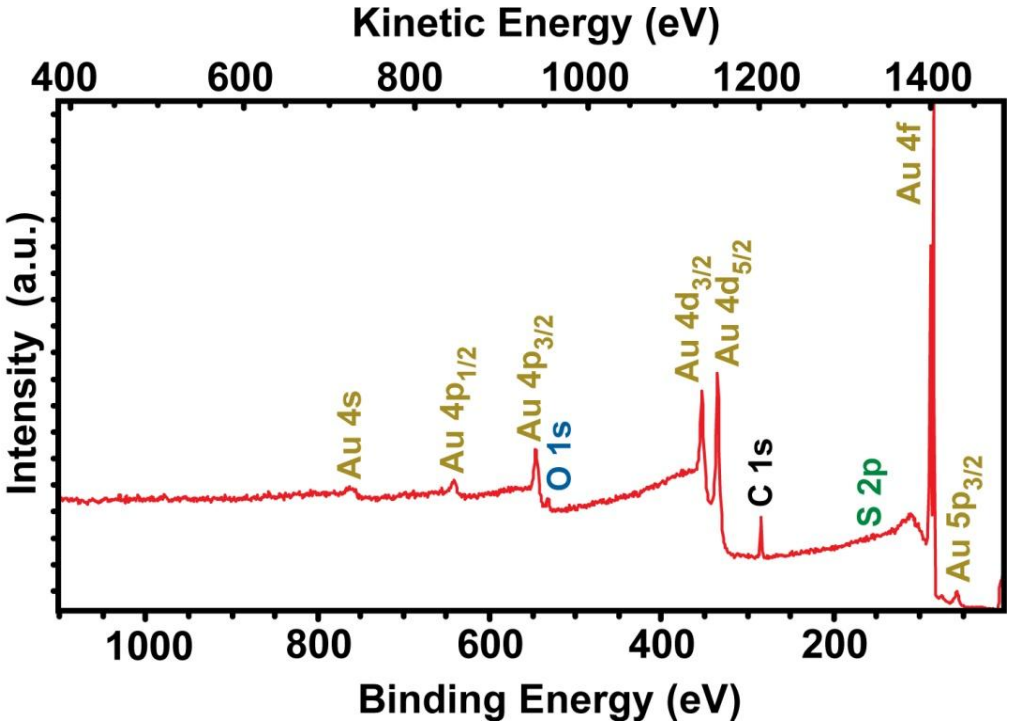

Figure 1.7: X-ray photoelectron survey spectrum of an **AD** SAM deposited from solution. Note that every peak is directly associated with an atomic orbital. Also, the Au 4d peak has a doublet resulting from spin-state splitting induced by ionization.[38]

Chapter 2

Self-Assembly on Germanium(100)

2.1 Overview

The reign of silicon as the leading semiconductor material in electronic applications may be nearing its end - a result of advances in dielectric film production. Other group IV semiconductors, because of their ability to function in a wide range of modern devices, provide the most capable replacements. Germanium has emerged as a candidate for future generations of fast, electronic devices, due to its high mobility and narrow bandgap.[7, 8, 10]

Germanium is presently found in few devices, a result of its poor native oxide. This oxide layer is poorly passivating, thermally unstable, and water soluble.[6, 25, 61, 62] When germanium is exposed to the atmosphere, a mixture of oxides, including GeO and GeO_2, form on its surface, in a process akin to oxidation of aluminum.[6, 62, 63] GeO_2 is an inferior dielectric and is water soluble.[6, 62] Both oxides suffer from instability. Further, the interface between germanium and its oxide is amorphous, and exhibits a significant amount of defects.[62] These features have limited germanium's utility and interchangeability with silicon. Figure 2.1 details the presence and solubility of the germanium oxide.

Techniques for the removal of germanium's oxide layer have been developed. Atomically clean surfaces have been achieved in ultrahigh vacuum (UHV) cleaning processes, but wet chemical techniques in ambient conditions are required for industrial purposes.[6, 62, 63] Although dielectric films have been successfully deposited onto clean

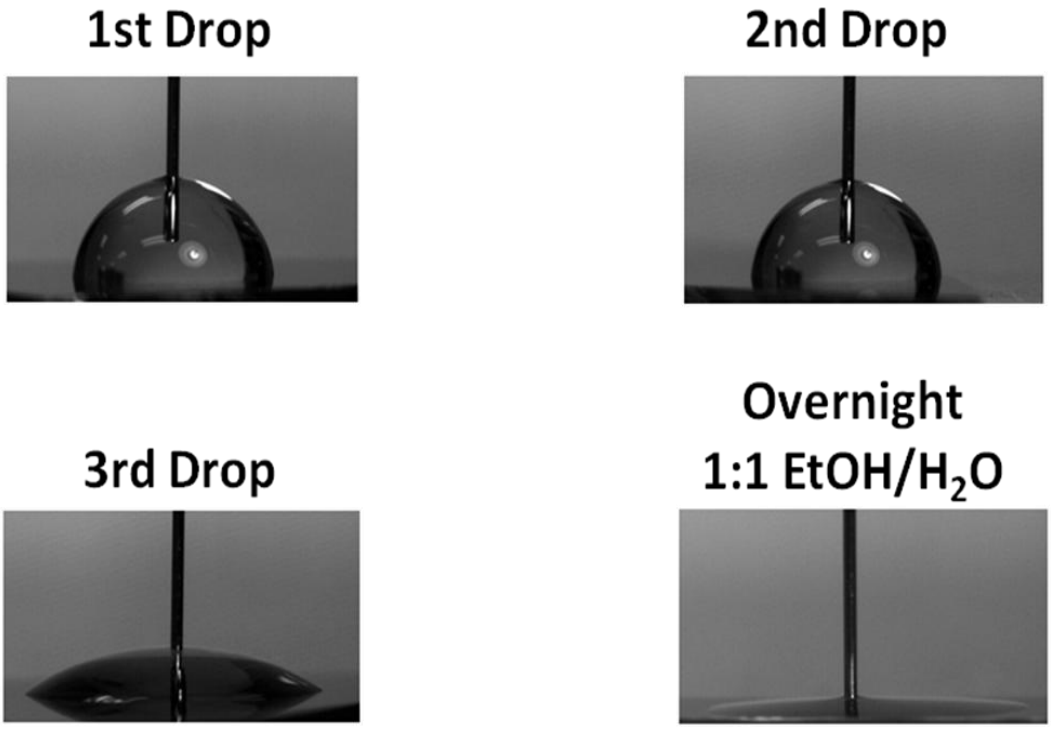

Figure 2.1: The dynamic surface of Ge(100). Illustration demonstrates the degradation of surface hydrophobicity as a result of oxide solubility. The first two drops represent a non-wetted surface caused by the presence of a germanium oxide layer. The third drop encountered the footprints of the previous two and expresses the true wetting ability of the germanium surface. The first drops actively removed the oxide layer and exposed the bare Ge(100) surface. The last image was taken on a surface exposed to a 1:1 EtOH/H_2O solution overnight, further displaying the solubility of the oxide layer.[64]

germanium surfaces, the interface characteristics of the interaction produce leaky and undesirable devices.[6] Until this point, it has been shown that removal of the oxide layer alone is insufficient for quality electronic performance, and for this reason, the cultivation of passivation techniques of germanium must be developed for production of functional components.[6]

2.2 Previous Work on Germanium

Germanium passivation is a topic of growing interest. Strategies involving hydrogen, halogen, sulfide, and alkyl passivation have been examined.[25] As described in chapter 1, alkanethiols have the ability to form well-ordered SAMs on a variety of surfaces. Self-assembly on germanium will provide control of its interfacial properties and improve surface passivation.[6, 65-67]

Cullen and co-workers demonstrated germanium alkylation by Grignard reaction in the 1960s.[68] Forming a Ge-C bond protects the surface from ambient conditions. The surface was first chlorinated by exposure to hydrogen chloride and chlorine gases, followed by ethyl magnesium bromide introduction.[68] Later work focused on halogenation and sulphidization. Surfaces of semi-conductors are highly reactive, and oxidation occurs as the result of unsaturated dangling bonds. To stabilize the surface, Lu introduced the substrate to HCl, which satisfied the reactive dangling bonds with monochloride.[69] Germanium(111) surfaces were shown to exhibit stable chlorinated surfaces in ambient conditions by means of wet chemical exposure to HCl.[69] Other studies have investigated the use of sulfur as a passivating agent.[70-72] The interaction of

sulfur and germanium breaks down surface dimers on the Ge substrate, allowing sulfur to adsorb at the interface and form a (1 ×1) reconstruction.[70-72] Germanium in various oxidation states were shown to remain on the reconstructed surface, however, leading to non-ideal surface properties. Recently, the deposition of alkyl chains on germanium has re-emerged as a useful technique for producing ideal surface conditions. The direct Ge-S bond leads to well-ordered monolayers giving good coverage and thermodynamic stability up to 450K.[6, 65, 73] The monolayer provides a means for surface passivation and offers the ability to modify surface properties and to integrate biological functionalities into solid-state devices. Current methods for SAM deposition on germanium involve multi-step processes, where oxide removal, passivation, and deposition all occur separately.[6] Existing procedures have exhibited the ability of alkanethiols to react readily with reactive sites on Ge(111) and Ge(100), producing stable monolayers.[6, 65, 66, 73]

2.3 Experimental Methods

Recent studies have shown that the deposition of alkanethiols on germanium is a reproducible process resulting in monolayers on technologically relevant substrates. Furthermore, the interaction between thiol solution and Ge(100) has been shown to construct a monolayer with superior stability and thickness to those on Ge(111).[6] Through control of reaction conditions, we have improved upon pre-established methods for alkanethiol self-assembly on Ge(100) and succeeded in simplifying the procedure.

2.3.1 Materials

Germanium(100) samples were purchased from Silicon Quest International (Santa Clara, CA). They were 350-400 μm thick and had resistivities of 40 Ω-cm. Absolute pure ethanol and 1-dodecanethiol (**C12**) were acquired from Sigma Aldrich (St. Louis, MO). Deionized water at 18.2 MΩ-cm resistivity was provided by a Milli-Q system from the Millipore Corporation (Bellerica, MA).

2.3.2 Fabrication of Monolayers

Solutions are made via a two-step process for all measurements. A 1 mM ethanolic solution of **C12** is prepared, which is then diluted with 18.2 MΩ-cm water, resulting in a 0.5 mM **C12** solution. The ethanol and water ratio is 1:1, unless otherwise specified. In cases where the ratio was varied, a measured quantity of **C12** was dissolved in ethanol, and then diluted with water to the specified volume, while **C12** concentration was kept at 0.5 mM. Adding **C12** to a pre-prepared ethanol/water solution can produce monolayers in many cases, but as **C12** becomes less soluble in the mixture, phase separation decreases reproducibility. Our procedure is preferable, because it ensures the dissolution of **C12** over a wide range of solvent ratios.

Samples of germanium, on the order of 9 mm^2 in area, were cleaved from a Ge(100) wafer along its crystallographic planes. The sample size was determined such that three separate contact drops could be placed on the surface without encountering a previously tested region. The samples were placed in a vial with the ethanolic solution and left alone for a pre-determined amount of time. A 24 hour deposition time can be

assumed unless otherwise specified. Samples were removed from the solution, rinsed with ethanol, blown dry with nitrogen gas, and placed in a clean vial until needed.

2.3.3 Volcano, Kinetics, and Stability Measurements

To decipher the role water plays in the deposition process, we ran a series of measurements with varying ratios between water and ethanol. Solutions of **C12** in the solvent/water mixtures were created for all desired ratios. Germanium samples were placed into each solution for 24 hours, and were analyzed by contact angle measurement.

To analyze the timescale of self-assembly between **C12** and Ge(100), we measured the contact angle for samples experiencing varying deposition times. A germanium sample is placed in a 1:1 solution of water/ethanol overnight to remove its oxide layer. It is rinsed, dried, and placed into a 0.5 mM solution of **C12** in a 1:1 mixture of water/ethanol for a time interval. The sample is removed, rinsed, dried, and analyzed. It is placed back into solution until the next time interval is reached. This procedure is repeated at specific time intervals for the remainder of the experiment.

Alkanethiolate SAMs will degrade over time if exposed to ambient conditions. It was suggested by Bent and co-workers that exposure to light accelerates the degradation process.[6] We tested this claim by monitoring contact angle stability on identically prepared samples, protecting some from light exposure while exposing others to light. An ethanolic solution of **C12** was prepared with a 1:1 ratio of water/ethanol and a 0.5 mM concentration. Germanium samples, cleaved from a single wafer, were placed into the solution for 24 hours, before being removed, rinsed, and blown dry. Initial contact angle measurements were taken. Both samples were placed in transparent glass containers; one

was left as is, while the other was covered in foil. Every 24 hours, the samples were removed, rinsed with ethanol, blown dry, evaluated through contact angle analysis, and then placed back into their respective vials.

2.3.4 Contact Angle Measurements

Our measurements were collected using a custom-built goniometer, encompassing a 0.50× magnification, 94 mm focal length InfiniStix (Hitachi Ltd., Tokyo, Japan) CCD camera. A flat-tip syringe-needle (33 gauge) is attached to a .2 mL Gilmont micrometer syringe (Cole-Parmer, Vernon Hills, IL) by means of Torr Seal (Varian, Inc., Palo Alto, CA) epoxy. Data were acquired by National Instruments (Austin, TX) Measurement and Automation software. Angles were measured using ImageJ software from Scion Image (Frederick, MD).

We chose to report advancing and receding angles separately, rather than reporting an equilibrium angle. The first step in our procedure was to deposit a 5 μL droplet of deionized water onto our sample surface. The needle was re-positioned to the center of the drop carefully, as to not disrupt its shape. The drop's volume was increased to 10 μL. An image of the droplet was recorded. Next, the droplet was expanded until the wetted area of the surface increased. The value for which this typically occurred was between 15-20 μL. Again, the needle was centered in the drop. The volume was reduced to 10 μL, and again photographed. This procedure was repeated for three separate locations on the sample surface to account for any physical or chemical heterogeneity. The initial image was analyzed as the advancing angle, and the latter image as the receding angle. Contact angles from both the left and right sides of the droplet were

measured and averaged together, resulting in that angle's value. The averages of the three advancing and receding angles were averaged and resulted in one advancing and one receding value for each substrate. Figure 2.2 illustrates the measurement procedure incrementally.

2.3.5 X-Ray Photoelectron Spectroscopy Analysis

Samples submitted for XPS analysis were kept in solution until being loaded into the XPS chamber. The base pressure of the chamber was set at 1×10^{-9} Torr. The samples were analyzed by a Kratos Axis Ultra photoelectron spectrometer using a monochromatic Al Kα (20 Ma, 14 kV) source and using a 300 μm × 700 μm spot size. Survey spectra were analyzed using a pass energy of 80eV (1 eV resolution) and high-resolution spectra of the Ge 3d, Ge 2p, C 1s, O 1s, and S 2p by a pass energy of 20 eV (0.1 eV resolution). The spectra peaks were fit using Gaussian-Lorentzian (GL) line shapes and a Shirley background in CasaXPS analysis software.[60, 74]

2.4 Results and Discussion

Self-assembly on germanium can occur in ambient conditions only in the absence of its native oxide layer. To accomplish this, previous work has demonstrated the success of a multi-step process. The procedure includes separate phases for removing oxide layers, passivating the surface against re-oxidation, and the deposition of alkanethiols. The oxide layer is water soluble and is removed by rinsing the surface with H_2O.[6] Passivation of germanium is accomplished by deposition of halogen atoms, as well as by treatment with chlorine or bromine, by means of hydrochloric or hydrobromic acid,

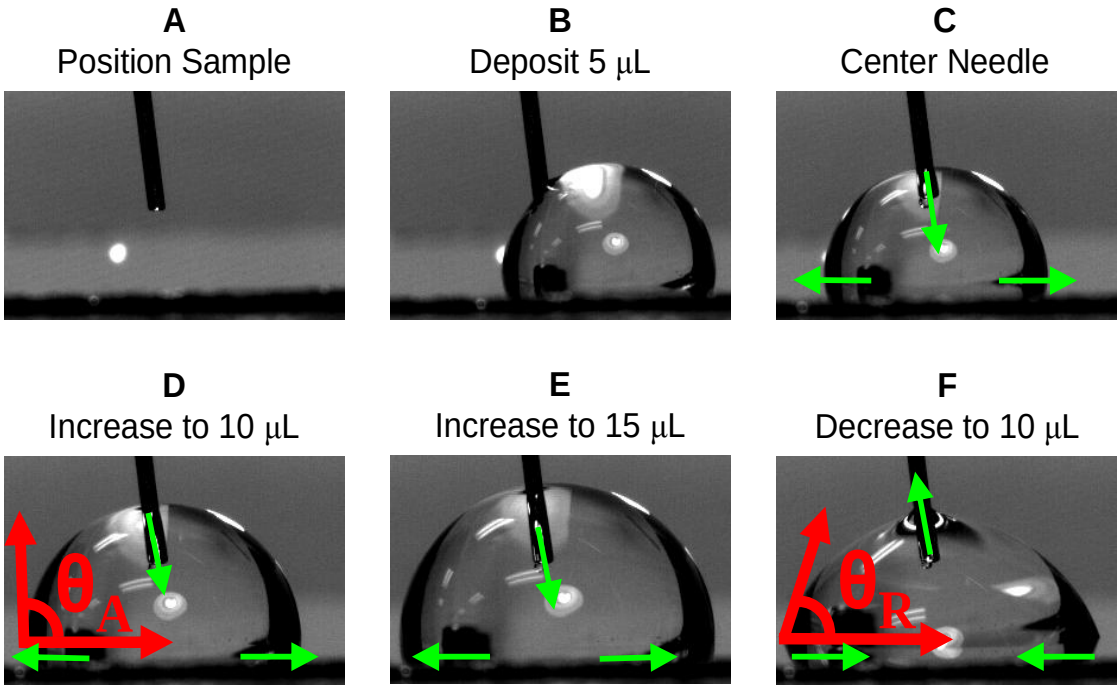

Figure 2.2: Step-by-step method of measuring contact angles by the dynamic sessile drop method. **A.** Syringe is located over an un-tested region. **B.** A 5 μL drop is deposited onto the substrate surface. **C.** The syringe is carefully centered within the drop. **D.** The drop volume is increased to 10 μL, and the advancing angle measurement is taken. **E.** The drop volume is increased to 15 μL (or until the wetted surface in increased). **F.** The drop volume is decreased to 10 μL; the receding angle is measured.[47]

respectively.[6, 65, 73] Hydrogen-terminated surfaces are formed from treatment with hydrofluoric acid. Passivating the surface slows down the re-oxidation process, allowing sufficient time for thiol deposition, before oxide reformation. It is critical to note that SAM deposition is dependent upon the absence of its native oxide, and not the presence of a passivating layer.

We introduce a process where removal of the oxide layer and self-assembly occur simultaneously, in the absence of a pre-formed passivation layer. The native oxide layer on germanium and the alkanethiol adsorbate have conflicting solubilities. Germanium oxide is soluble in water, but not in ethyl alcohol. Alkanethiols fail to produce homogenous mixtures in water, but will do so if mixed in ethyl alcohol. By mixing water and ethanol, we produce an environment for which both the adsorbate and oxide layer are soluble. This solution can dissolve the oxide layer, and enable deposition in a single step. Alkanethiol SAM formation cannot occur successfully if the oxide layer fails to be completely removed, or if the adsorbate is insoluble. Therefore, alcohol and water are both necessary constituents in the thiol solution. Figure 2.3 shows our method for **C12** SAM deposition on germanium.

2.4.1 Mixed-Solvent System

We designed an experiment that would yield insight into both the ability of self-assembly to occur in a mixed-solvent environment, and which water/alcohol ratios would satisfy both oxide and thiol solubility. We analyzed mixtures between water and three solvents; ethanol, methanol and *t*-butanol. Figure 2.4 shows "volcano plots," expressing the relationship between solvent/water ratio and the SAM quality. The *t*-butanol data is

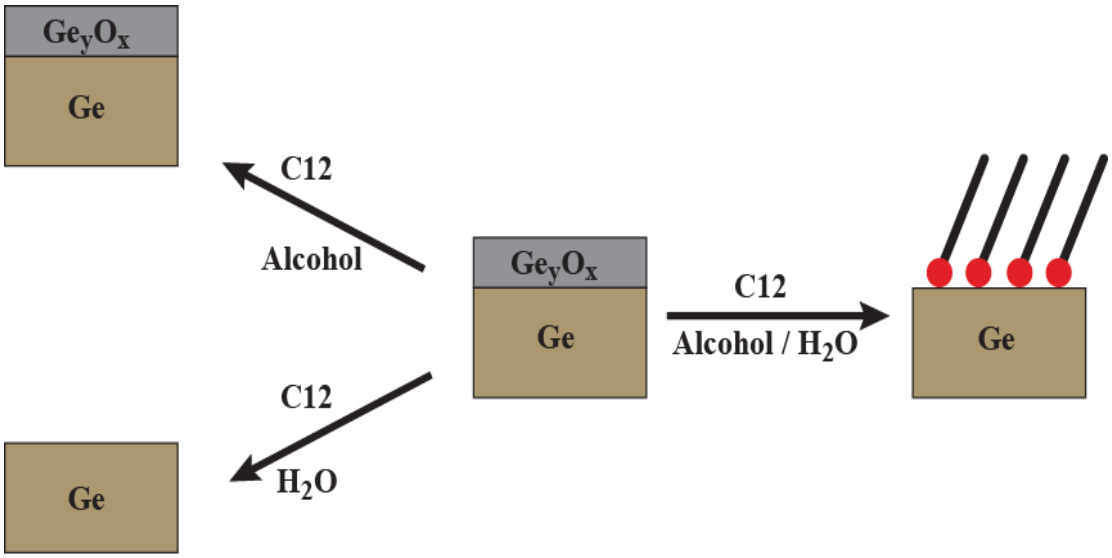

Figure 2.3: The importance of solubility on direct SAM deposition on Ge(100). Germanium oxide is soluble in water, while the alkanethiols are soluble in alcohols. A water/alcohol mixture can solvate both the germanium oxide and enough alkanethiol to form full-coverage SAMs. The unmixed solvents (and exposure in a stepwise fashion) do not produce SAMs.[25]

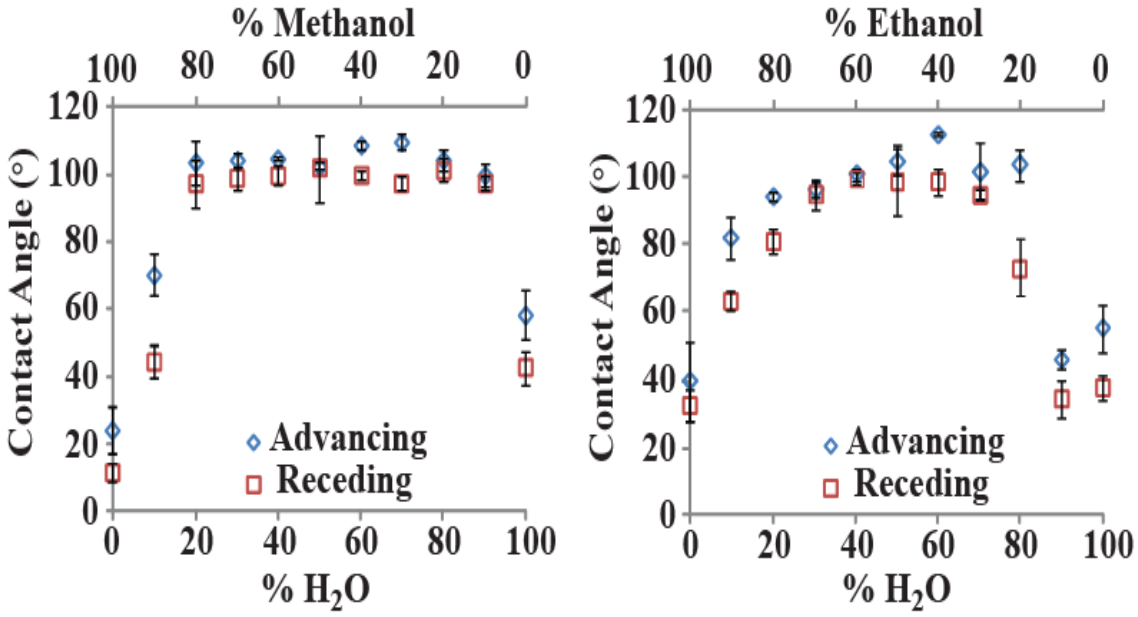

Figure 2.4: Dependence of SAM quality on mixed solvent ratio. The appropriate quantity of **C12** is dissolved in the ethanol fraction, and then diluted with water to the selected volume and ratio. Methanol yields a wider window of solvent composition than ethanol. Films with an advancing contact angle greater than 100° are considered to be of high quality. *t*-Butanol results are not shown, as no ratio resulted in complete films.[25]

not shown as it failed to produce any complete films. Advancing contact angles equal to or greater than 100° are considered to be indicative of good monolayer coverage, and a quality SAM.[75, 76] Quality monolayers were formed for a methanolic solution containing 20-80% water. Ethanol only produced good SAMs for water percentages between 40% and 60%. Methanolic solutions exhibited the ability to out produce ethanolic counterparts for both the case of low and high water concentrations. We propose that in low water/high alcohol situations, germanium oxides are more soluble in mixtures containing methanol rather than ethanol or *t*-butanol. Higher solubility allows complete removal of the native oxide layer and drives self-assembly. Intuition would suggest that for high water mixtures, self-assembly would improve for an increase in alcohol hydrophobicity, due to the hydrophobic alcohol's ability to keep alkanethiols solvated. However, the data showed that the more hydrophobic alcohols, ethanol and *t*-butanol, failed to form SAMs under these conditions. We believe that these results suggest a deposition process dependent upon more than simple solubility, and further study will be required to determine the mechanism.

2.4.2 Deposition Kinetics

The coverage and quality of monolayer films can be tracked by contact angle measurements, enabling the study of the relationship between the growth of a SAM and its solution exposure time. It is accepted that full-coverage *n*-alkanethiol SAMs produce contact angles of ≥100°.[75, 76] Contact angle measurements on bare, as-received germanium are affected by the instability, and presence of a native oxide layer. In the case of virgin contact between water and germanium, contact angles are indicative of the

hydrophobic nature of GeO and GeO_2. Additional drops, as a result of oxide removal, will begin to exhibit the strongly hydrophilic characteristics of a pure Ge(100) surface. This phenomenon is shown in Figure 2.1. Short solution exposure times were inadequate for removal of the oxide layer. Before kinetics measurements were taken, to ensure that the pure germanium surface was being studied, the sample was introduced to a 1:1 water/ethanol solution for 24 hours. By stripping the oxide layer, any increase in hydrophobicity can be attributed to the deposition of **C12**. Figure 2.5 shows the growth of a monolayer on germanium with time. A period of rapid growth occurs between 10 and 1000 minutes, with little to no improvement in monolayer quality after 24 hours. High coverage films are observed after 6-18 hours. Self-assembly on germanium is a slow process in comparison to gold, where alkanethiolates achieve full coverage within seconds.[12] The time for full coverage to occur varied between runs, but complete monolayers were achieved within 24 hours for all cases.

2.4.3 Long Term Stability

Self-assembled monolayers will degrade over time if not protected from ambient conditions. Our one-pot synthesis method for depositing SAMs on germanium produced monolayers with stability characteristics comparable to those reported in previous work, leading us to suspect that the degradation process will also be similar. Bent and co-workers suggest that defects or impurities in the monolayer allow ambient oxygen to interact with the germanium surface, and cause re-oxidation.[6] Our measurements are consistent with this suggestion. Once the oxygen accesses the substrate and initiates re-oxidation, the SAM loses its ability to protect the surface. Degradation occurs until the

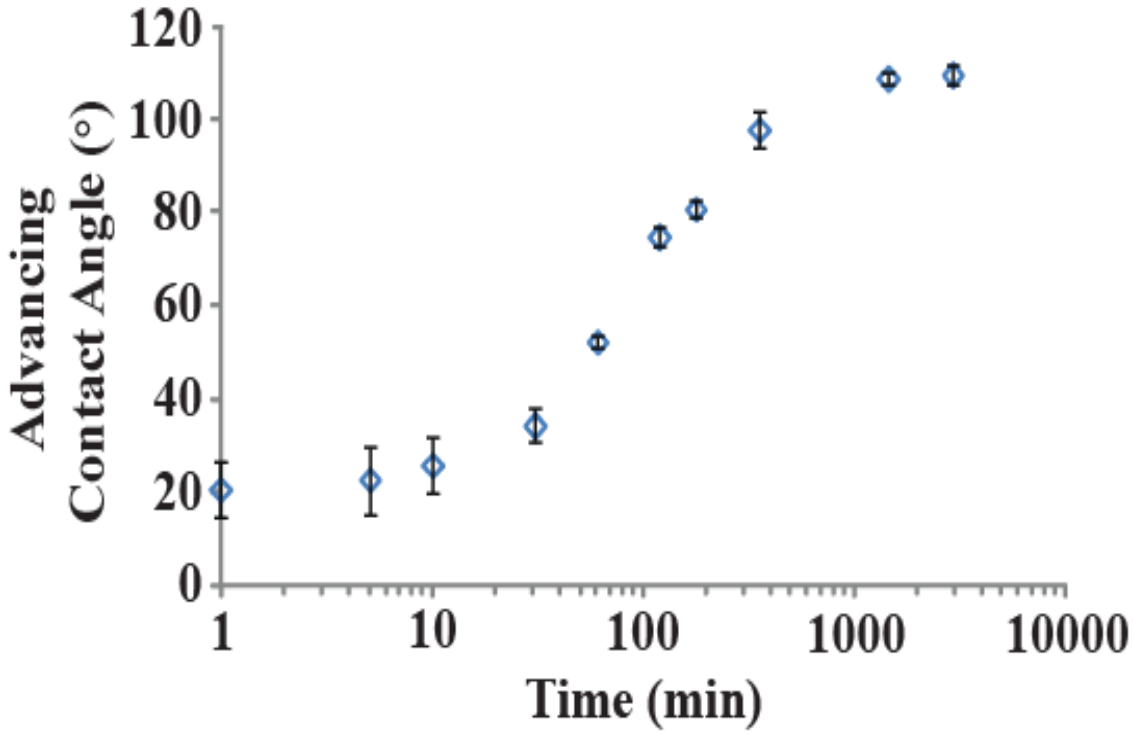

Figure 2.5: Kinetics of SAM formation on Ge(100). Deposition is from 0.5 mM **C12** solution in 1:1 ethanol/water. Advancing water contact angles are shown on the logarithmic scale for clarity. The period of most dramatic change occurs between 10 and 1000 min., and run-to-run variation occurs in this region.[25]

entire surface is once again covered in an oxide film similar to that of the as-received sample. Bent also suggested that exposure to light caused the monolayer to degrade more rapidly.[6] To test this claim, we exposed samples of identical preparation parameters to ambient conditions. One sample was exposed to light, and the other confined to darkness. Figure 2.6 shows our data for the degradation of monolayers in relation to varying light conditions. Degradation is present in both cases, but no significant differences in the rate of re-oxidation are apparent. This leads us to believe that mild light exposure has little bearing on the process, and that defects in the monolayer are the dominant factor for re-oxidation rate.

2.4.4 X-Ray Photoelectron Spectroscopy Analysis

X-ray photoelectron spectroscopy analysis is used to confirm the formation of SAMs on germanium and the presence/removal of germanium oxide. Figure 2.7 shows the high-resolution spectra of the C 1s, S 2p, Ge 2p, Ge 3d, and O 1s orbitals. These spectra are intrinsic to the elements we wish to identify. Carbon and sulfur are indicative of the **C12** monolayer. Germanium and oxygen provide substrate information. Each individual spectra is overlaid with three peaks representing the as-received germanium sample (black trace), the oxide-free, bare Ge sample (blue trace) produced from rinsing in 1:1 water/ethanol solution, and SAM sample (red trace).

The C 1s and S 2p spectra will be discussed first. As expected, the as-received germanium sample exhibits a broad carbon peak. The majority of adventitious carbon is adsorbed on the germanium oxide. Removing the oxide layer also acts to rid the surface

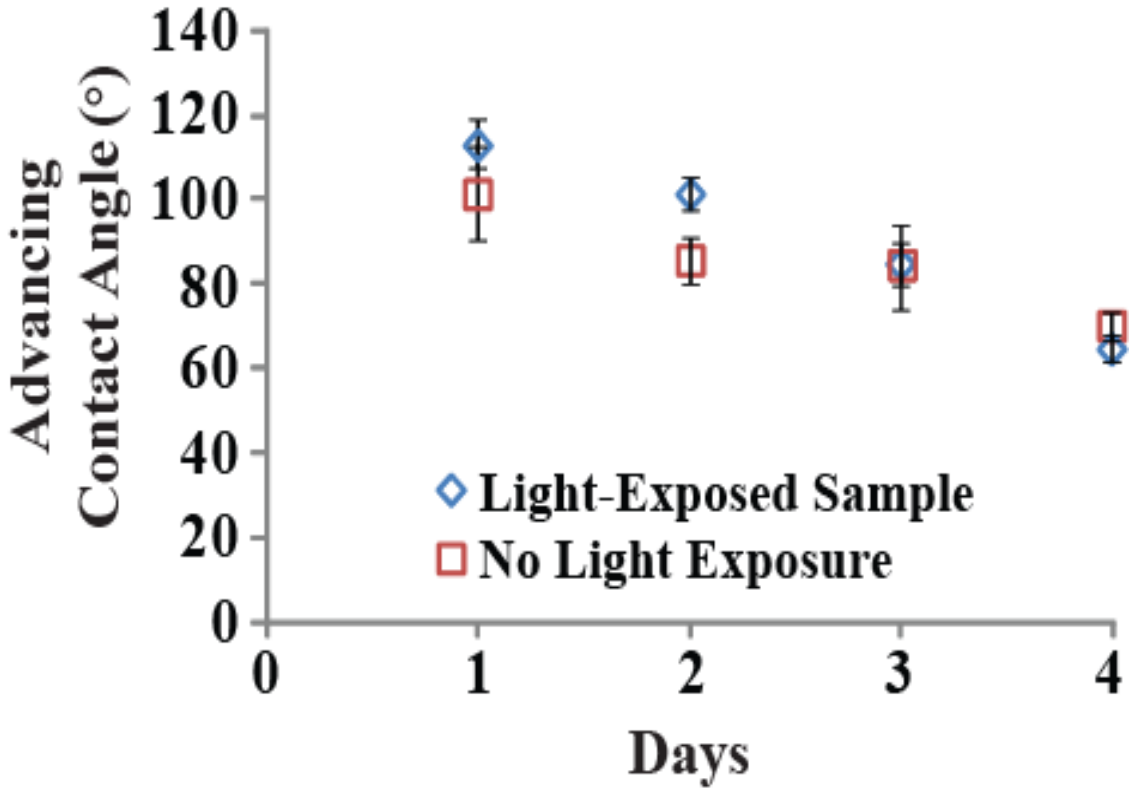

Figure 2.6: Advancing contact angles collected after days of exposing **C12** SAMs on Ge(100) to the ambient environment, with samples either exposed to or protected from light. There was no significant difference between the two series.[25]

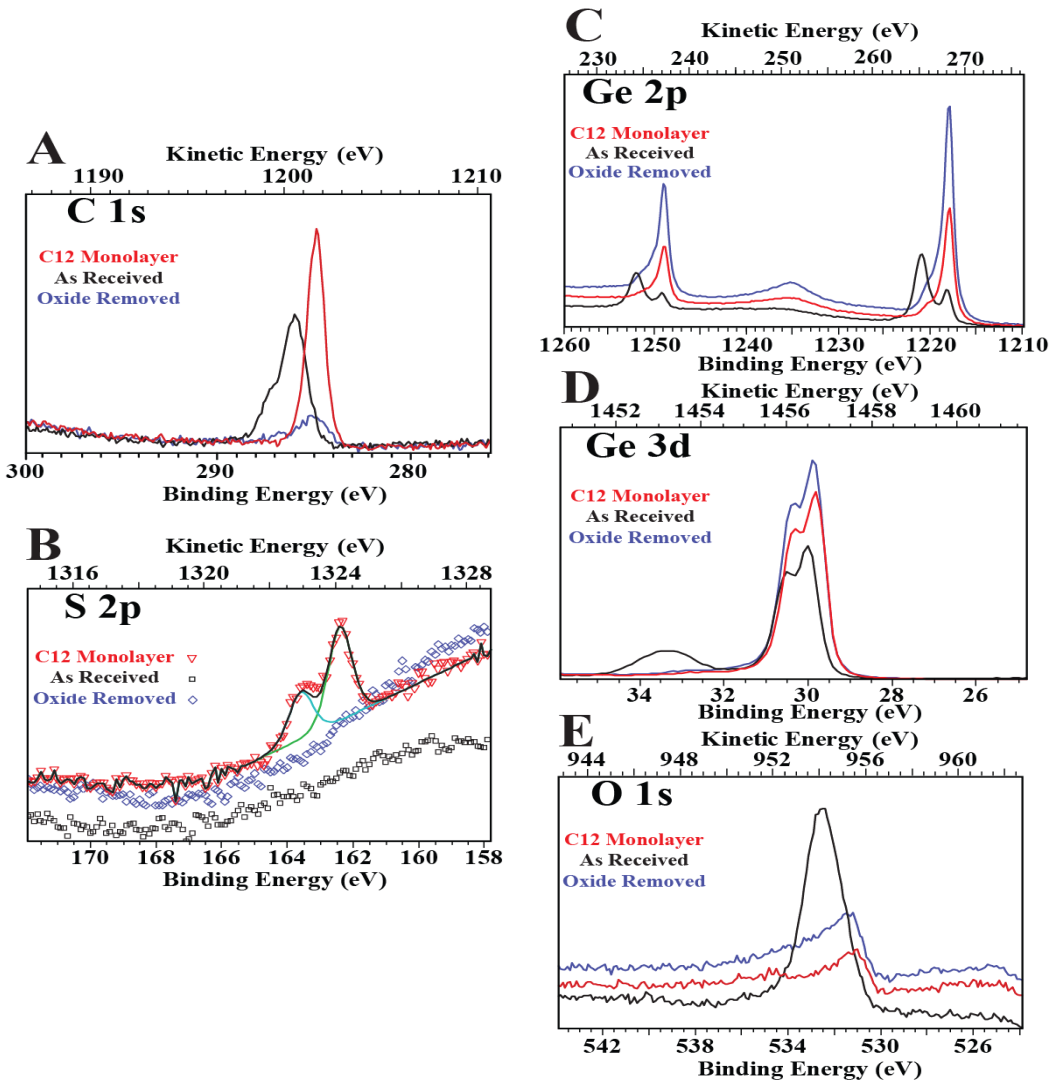

Figure 2.7: High-resolution XPS spectra collected for the regions specific to the C 1s, S 2p, Ge 3d, O 1s, and Ge 2p. Each region is shown with its own arbitrary intensity scale. **A.** Adventitious carbon (black trace) is effectively eliminated by treatment with the water/ethanol (blue trace), enabling a high-purity **C12** SAM to form (red trace). **B.** The **C12** monolayer gives the expected response in the S 2p region, while the as-received and the cleaned wafers do not show the presence of any sulfur. **C.** Oxidized species (red trace) are removed readily by the water/ethanol treatment, leaving high intensity peaks attributed to the bulk germanium crystal (blue trace). The intensity is attenuated by the presence of the SAM (red trace). **D.** The Ge 3d spectra provide information complimentary to that of the Ge 2p spectra. Water treatment again eliminates the signal from the oxidized Ge species (blue trace). The Ge 3d doublet appears shifted slightly to a lower binding energy. The intensity is again attenuated by the presence of the monolayer (red trace). **E.** The majority of the oxygen is attributed to the native germanium oxide; after removal or SAM formation, remaining oxygen is attributed to residual alcohols or oxide reformation at defect sites before the samples were loaded into the XPS vacuum chamber.[25]

of carbon contamination, evident by the absence of a strong carbon signal for the bare Ge sample. The SAM sample exhibits a sharp peak at 284.9 eV, typical of carbon atoms in a **C12** monolayer.[77, 78] The direct Ge-S bond formed by alkanethiol self-assembly on germanium is represented by the S $2p_{3/2}$ and S $2p_{1/2}$ peaks, at 162.4 and 163.6 eV, respectively. The presence of the aforementioned sulfur peak, and the lack of sulfur signatures for the other germanium samples is in agreement with spectra measured for thiolates on gold.[75, 78-80]

The Ge 2p, Ge 3d, and O 1s peaks inherent to germanium and its oxide will now be discussed. The variation in the Ge $2p_{3/2}$ and Ge $2p_{1/2}$ peak intensities are indicative of the progression of the self-assembly formation procedure. Both bulk germanium (1218.0 and 1249.0 eV) and oxidized germanium (1220.9 and 1252.0 eV) are present for the as-received sample.[63] The cleaned sample exhibits a strong reduction in the germanium oxide peaks and a growth in bulk germanium peaks. The decrease in the oxide peak suggests that the solvent/water mixture successfully removed the native oxide layer. The removal of the oxide layer provides photoelectrons generated in the bulk germanium an un-inhibited pathway to the detector, explaining the dramatic increased peak intensity. The remainder of a germanium oxide peak is attributed to the brief ambient exposure the sample receives before loading in the vacuum chamber. The SAM sample again experiences a decrease in the bulk germanium peak intensity due to the thickness of the **C12** monolayer, blocking some photoelectrons from the bulk germanium. The degradation and short life times of SAMs on germanium can be attributed to the gradual growth of germanium oxide in defects of the SAM after assembly, shown to be present in the form of a weak shoulder at 1220.9 eV.

The Ge 3d region expresses similar characteristics to those of the 2p peak. The Ge 3d peak also experiences splitting in the form of the Ge $3d_{5/2}$ (29.95 eV) and Ge $3d_{3/2}$ (30.53 eV) doublet, but the peaks are not well-resolved.[63, 81, 82] The oxide layer appears in the form of GeO_2 with a peak at 33 eV in the as-received sample. The presence of oxide is negligible for both the cleaned surface and post-deposition samples. The Ge 3d peak experiences a slight shift to higher binding energy after the removal of its oxide layer, a result of passivation layer elimination. Again, the bulk germanium peak experiences a reduction in intensity after deposition occurs.

Finally, the O 1s peak exhibits a strong intensity at 532.5 eV for the as-received sample. Its intensity decreased, but some oxygen is still present after oxide removal and SAM deposition. This is attributed to reformation of oxide due to ambient exposure, to the presence of defect sites in the SAM, and to residual adsorption of ethanol.

2.5 Conclusions

We have demonstrated the ability to deposit well-formed alkanethiol monolayers on Ge(100) surfaces by a single-step deposition technique. The critical factor for successful deposition is the adjustment of the water/solvent mixture such that both the oxide layer and adsorbate species can be efficiently dissolved. Our ultimate goal is to produce a self-assembly technique for germanium that produces monolayers mimicking the advantages of those of thiols on gold. Alkanethiols on Au{111} present a model system for self-assembly for several reasons, particularly the ease with which quality films can be deposited. We propose that simple self-assembly can be extended to a number of substrates if the proper chemistries are developed.

Chapter 3

Chemical Patterning on Germanium(100)

3.1 Overview

The recently realized potential of micro- and nano-arrays on solid substrates has driven the trend of electronic miniaturization.[83, 84] Self-assembly is a powerful approach for nano-scale device construction. Recently, self-assembled monolayers have attracted increasing interest for their ability to interact with, and to control, interfacial chemistry of semiconductor substrates. The current challenge is the preparation and integration of thin films into semiconductor-based devices. Chemical patterning techniques, especially μCP, have been used to produce single-molecule-thick nanostructures with micron (or better) resolution on technological substrates, exploiting both the stable nature of SAMs and the ability to place individual molecules precisely.[50, 54, 85, 86] Patterning processes enable the fabrication of arrays and the manipulation of interfacial properties.

3.2 Previous Work: Chemical Patterning and Thin Film Deposition

Alkanethiols on gold are widely recognized as the model system for self-assembly. It follows that the majority of chemical patterning and film deposition techniques have been engineered to facilitate this chemistry. With the development of the integrated circuit, an ever-increasing need for solar energy, and a trend toward the miniaturization of electronic components, novel techniques for patterning on semiconductor substrates are desirable. Recently, research has begun to manipulate pattering techniques originally intended for thiols on gold, extending them to other materials. This emerging field has great growth potential. Some of the more prevalent

techniques for patterning on semiconductor substrates discussed in recent literature are worth examining to set the current work in perspective.

3.2.1 Vapor Deposition and Etching

Thin films can be used to stabilize semiconductor surface sites and to improve electrical properties, including carrier mobility and conductivity. Deposition of thin films is the most direct way to obtain high-κ dielectric layers on both silicon and germanium.[87] Not only are the creation of direct substrate/dielectric interfaces possible, but such thin films may act as the foundation for etching and lithography methods.

Vapor deposition is a frequently implemented technique for thin-film deposition. Vapor deposition techniques are categorized under two broad terms; chemical vapor deposition (CVD),[87-93] and physical vapor deposition (PVD).[90] The former depends on surface chemical reactions to deposit material, and the latter employs physical methods such as sputtering to construct films.[90] Chemical vapor deposition occurs in several forms; plasma-enhanced chemical vapor machining (CVM),[93] ultrahigh vacuum CVD (UHV-CVD),[92] low-pressure CVD (LPCVD),[91] and metal-organic CVD (MOCVD),[87] amongst others. Physical vapor deposition can also be found in many forms, including pulsed-laser deposition (PLD)[94] and sputter deposition.[90]

The ability to insert certain materials into electronic devices is first dependent upon thin-film deposition, with patterning a secondary concern. Vapor deposition is not a direct patterning technique, but it offers a method for growth of dielectric films on semiconductor substrates. The resultant films lend themselves to patterning procedures. Etching is a patterning technique often associated with thin films. It utilizes patterning

masks and chemical reactions to remove surface layers selectively.[92] Zanier and co-workers demonstrated the utility of electron-beam lithography for the patterning of square lattices of circular dots onto a photoresist. Resist dots were used as a master to transfer the pattern onto a SiGe substrate. Reactive ion etching (RIE) uses the gas mixture SF_6/CHF_3 to remove the top layers of the unmasked SiGe surface, leaving a periodic lattice of dots on the substrate.[92] Such RIE procedures are critical methods for the subtractive patterning of surfaces.[91-93, 95-97] Etching is also used to remove undesirable surface layers, so that functional adsorbates can be deposited.[6, 98-101] The mask designs and etching chemicals are varied in accordance with preferred patterns and materials. Etching meets requirements for both the ability to pattern on semiconductor substrates and production of nanometer features.[93, 95] Similar methodology will be revisited later in section 3.4, where we selectively remove germanium's native oxide prior to chemical patterning.

3.2.2 Additional Patterning Techniques for Semiconductors

A number of soft-lithography techniques have been used to create controllable microstructures, though feature sizes below 100 nm remains an important challenge.[86]

Dip-pen nanolithography (DPN) has been used to fabricate nanoscale features, and has recently moved beyond gold substrates and onto semiconducting and insulating materials.[85, 86, 102, 103] Dip-pen nanolithography utilizes an ink-soaked atomic force microscope (AFM) tip to direct-write (and thus to pattern) molecular adsorbates onto surfaces. Physical or chemical reactions between the ink-soaked tip and substrate cause materials to immobilize and to bind to the surface. Because the reaction occurs at the

AFM tip, material adsorption will localize along the tip's trace pattern.[86] In the case of standard DPN (as opposed to newly developed techniques, including electrochemical DPN), the ink is transported from the tip to the surface through a medium, typically a water meniscus.[85, 86, 103] This technique is excellent for the production of serially-produced features with sub-100 nm dimensions, even depositing line widths as small as ~10 nm.[85]

Wang and co-workers demonstrated the ability to grow and to pattern germanium nanowires on various substrates *via* a gold-seeded vapor liquid solid (VLS) technique.[88, 89] CVD was applied, using germane (GeH_4) gas, forming an alloy through the dissolution of germane into a Au cluster. Further exposure causes the alloy to liquefy, followed rapidly by the supersaturation and precipitation of the germanium, resulting in the axial growth of single-crystal nanowires.[88] They proposed two techniques for patterning the germanium nanowires onto substrates. First, e-beam lithography is used to pattern small arrays of Au atoms into islands. The islands will nucleate into ordered dots upon annealing. The germanium nanowire growth process can be performed on the Au dots.[88]

A second patterning technique involves germanium nanowire passivation and the use of Langmuir-Blodgett troughs to form ordered assemblies of the wires. Again, CVD was used to grow nanowires on silicon substrates. The nanowires were removed and cleansed *via* ultrasonification and etching, respectively.[89] The wires are passivated by alkanethiols through the use of a Grignard reaction. The passivated nanowires are placed into a Langmuir-Blodgett trough filled with an ethanol/water mixture, where they form a close-packed, dense film oriented parallel to the trough edges. From this state, the wires

can be transferred to many substrates.[89] Even if a non-semiconducting substrate is used, the sample will retain the semiconducting character of the germanium nanowires. Passivated germanium nanowires have exhibited the ability to endure patterning, offering an alternative route to device fabrication.

3.2.3 Microcontact Printing on Germanium

Microcontact printing is the technique utilized for patterning on germanium in this dissertation. As described earlier, it has potential for a wide range of microelectronic applications. We chose μCP for several reasons. Although traditional lithographic techniques have supplanted it for maximum resolution, it remains the pre-eminent method for producing well-ordered and stable chemical patterns with microscale features over long ranges. Secondly, μCP lends itself to the technique we devised for self-assembly on germanium in chapter 2. Finally, despite the large body of work for alkanethiol deposition on gold, there is comparatively little work on μCP of molecular inks on semiconductor substrates.[104]

Wang and co-workers successfully deposited nanometer-scale patterns of SAMs onto amorphous Si, crystalline Si, and SiO_2 substrates, by means of μCP.[104] Their simple methodology employed a patterned polydimethylsiloxane elastomeric stamp, a octadecyltrichlorosilane (**OTS**) molecular ink, and the use of potassium hydroxide for etching. They provide a demonstration confirming that μCP on semiconductor surfaces is possible. In each of these cases, silane reacts with the native silicon oxide, a robust oxide.

Patterning on germanium, however, is complicated by its native oxide layer. Recall from the previous chapter that the water soluble and unstable germanium oxide

precludes the use of strategies akin to those employed on silicon. As a result, there are no reports of direct chemical patterning of molecular inks on germanium by μCP in the literature. Modifications to the microcontact printing procedure have been developed, however. Porter and co-workers demonstrated a method for negative patterning of thin Au, Pd, and Pt nanoparticle films on Ge(100), by μCP.[83] They present a negative μCP technique in which an aqueous solution of metal salt is placed onto a germanium surface and patterned by a **PDMS** stamp. A solution of $PdCl_4^{2-}$ was dropped onto the germanium surface and immediately contacted by an oxidized, hydrophilic **PDMS** stamp.[83] The salts undergo slow re-oxidation, resulting in spatially defined features of metal particles, located in non-contact regions.

3.3 Experimental Methods

There exists a disproportionate relationship between the importance of patterning on germanium and the amount of work devoted to studying it. Application of soft lithography techniques has significant potential for the development of new devices. By manipulating standard μCP procedures, we have developed a method that enables us both to remove germanium's native oxide layer and to deposit alkanethiol SAMs, simultaneously.

3.3.1 Materials

Germanium(100) and silicon(100) wafers were purchased from Silicon Quest International (Santa Clara, CA). They were 350-400 μm thick and had resistivities of 40 Ω-cm. Absolute ethanol, 11-mercaptoundecanoic acid (**MUDA**), and 1-dodecanethiol

were acquired from Sigma Aldrich (St. Louis, MO). Deionized water at 18.2 MΩ-cm resistivity was provided by a Milli-Q system from the Millipore Corporation (Bellerica, MA). Hydrochloric acid of 36.46 molar mass was acquired from EMD Chemicals, Inc. (Gibbstown, NJ). Polydimethylsiloxane stamps were produced in-house, using **PDMS** Sylgard 184 base and **PDMS** Sylgard 184 cure (Dow Corning, Midland, MI).

3.3.2 Stamp Preparation

The **PDMS** polymer was made in accordance with procedures described elsewhere.[105] Stamps were patterned using Si/SiO_2 masters. Micron-scale relief features on the master were generated using photolithography and reactive-ion etching. Before stamp production, the silicon master was covered with trichlorosilane to inhibit **PDMS** adhesion.[105] The polymer was poured onto the master, and subsequently degassed in a vacuum until all air bubbles were removed. The **PDMS** was placed in an oven, set to 90°C, for 2 hours.

A 25 mM ethanolic solution of **C12** was prepared. **PDMS** stamps were placed in the solution overnight, allowing alkanethiols to diffuse into the stamp. The **PDMS** stamps were removed from the solution, rinsed and blown dry. The stamps were placed into a beaker containing a 1:1 water/ethanol solution. They were arranged such that the patterned faces were fully exposed to the solution. The stamps were ultrasonicated for three minutes to remove surface contamination. They were removed from the sonicator, rinsed, and blown dry.

Just before use, the stamps were further cleaned by a blotting technique. A silicon wafer was treated in an ultraviolet (UV)-ozone oxidation cleaner (UV clean model

135500, Boekel Scientific, Feasterville, PA) for ten minutes to prepare the clean silicon surface for blotting. The stamp was blotted by mechanically pressing the patterned face against a virgin region of the silicon wafer. After careful removal (making sure not to touch the blotted face) from the silicon surface, the stamp was ready for printing.

3.3.3 Sample Preparation

Samples of germanium were cleaved from a Ge(100) wafer along its crystallographic planes. The samples were placed in a 1:1 water/ethanol solution overnight. They were removed, rinsed with neat ethanol, blown dry with nitrogen, and placed in a petri dish, making sure the polished germanium surface was facing upward. For submerged μCP (SμCP), water at 18.2 MΩ-cm resistivity was added to the petri dish so as to submerge the sample completely. The sample remained undisturbed for at least 10 minutes.

3.3.4 Stamping Procedure

The **PDMS** stamp was placed on top of the prepared sample such that the patterned side of the stamp and the polished face of the sample were in contact. A weight was placed on top of the stamp to ensure conformal contact between it and the sample for the duration of the experiment. When the desired stamping time interval was met, the samples were removed from the petri dish, peeled from the stamp, rinsed with ethanol, blown dry, and placed in a clean vial until analysis.

For backfilling, samples prepared at 24 hour stamping intervals were submerged in a 0.5 mM 1:1 ethanol/water solution of **MUDA** for 24 hours. The sample were

removed from solution, rinsed, blown dry, and placed into a clean container, until scanning electron microscopy (SEM) analysis.

3.3.5 Analysis Techniques (XPS, SEM)

X-ray photoelectron spectroscopy measurements were performed to determine the coverage of μCP SAMs on germanium. Samples submitted for XPS analysis were produced from time-dependent experiments, described below. Because these samples could not be replaced into solution after termination of stamping, the procedure was carefully formulated to minimize the time between removal from solution and XPS analysis. The order of the experiments was arranged such that sample requiring maximum stamping time was initiated first, followed by the next longest exposure, such that all runs would conclude at approximately the same time. The XPS analysis procedure is identical to the measurements performed in chapter 2. For this experiment, only the C 1s region is reported, as the results from the other regions are similar to what was already shown.

Scanning electron microscope images were used to determine the stamping mechanism's ability to transfer pattern features. Field-emission scanning electron microscopy (FESEM) images were collected using a LEO 1530 Gemini System (Carl Zeiss, Inc., Oberkochen, Germany). The system was maintained at an operating voltage of 5 kV. Primary electron-beam currents of 125 pA at 1 kV were used to collect images, utilizing an in-lens secondary electron detector. Sample exposure to the e-beam was limited to no more than 20 s to limit sample damage. The electron detector was maintained at a collection voltage of +300 V, with an aperture size of 30 μm.

3.4 Results and Discussion

Microcontact printing has the ability to produce well-ordered and stable SAM patterns of microscale features[50], but little work has been done to test its applicability on germanium. The lack of patterning work on germanium can be attributed to an intrinsic oxide layer that resists pattern deposition. In chapter 2, we detailed a method for successful formation of monolayers through concurrent alkanethiol deposition and oxide layer removal. Manipulation of μCP, in the form of SμCP, enabled us to reproduce those results, demonstrating a μCP technique directly applicable to germanium.

3.4.1 Technique Progression

To test the ability of μCP to transfer pattern features and produce full-coverage monolayers on germanium, we analyzed samples with XPS and SEM. Because XPS is an ensemble technique, unpatterned (flat) stamps were used for monolayer deposition, so as to create a uniform surface. First, we performed μCP on as-received germanium. This method failed to produce a monolayer. A second sample was introduced to a water bath, and stamped in the presence of the water medium, described schematically in Figure 3.1. This submerged microcontact printing technique was utilized so as to remove the native oxide layer and inhibit reoxidation.[106] We attempted to improve the technique by submerging the germanium in hydrochloric acid (HCl).

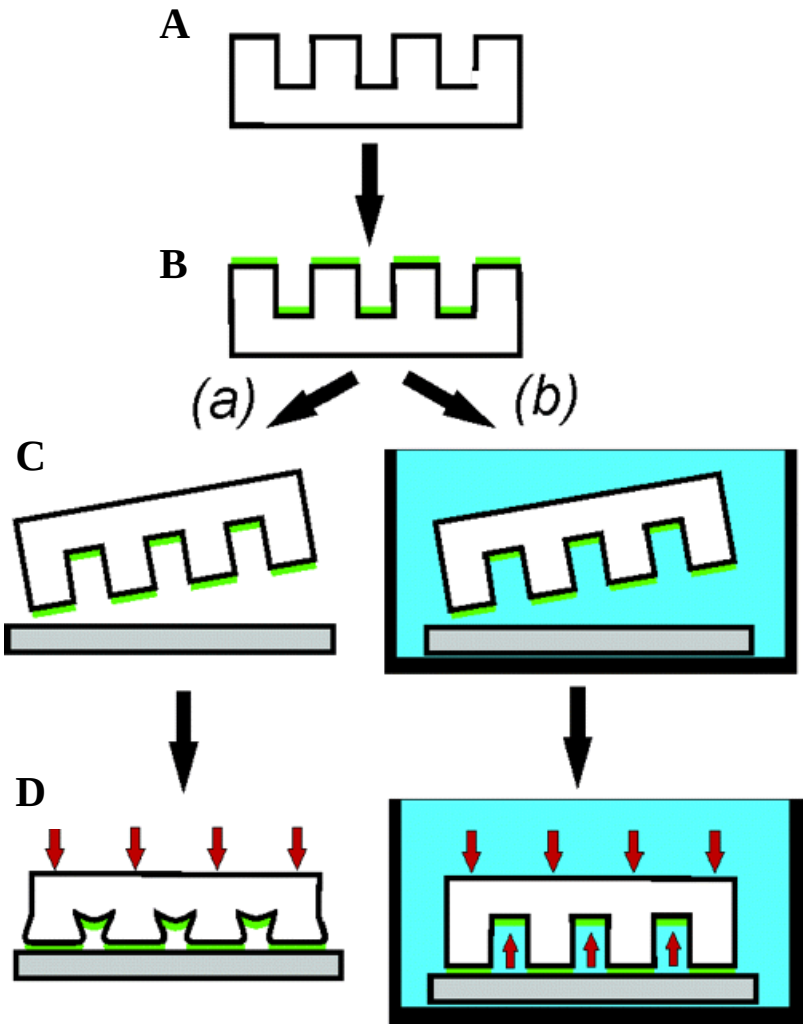

Figure 3.1: Schematic comparing standard microcontact printing (a) and submerged microcontact printing (b). **A. PDMS** stamp is produced through introduction to an etched silicon wafer. **B.** The stamp is saturated by an ethanolic **C12** solution. **C.** In standard microcontact printing, the stamp is mechanically pressed against the substrate under ambient conditions. Our method involved contact between stamp and germanium in the presence of water, so as to eliminate the native oxide. **D.** Adsorbate pattern is deposited onto substrate in atmospheric air (a), and while submerged in water (b).[106]

3.4.2 X-Ray Photoelectron Spectroscopy Analysis

As was addressed in chapter 2, the photoelectrons generated by the carbon atoms of alkyl chains exhibit a binding energy of 284.9 eV. The intensity of that peak corresponds to the population of the **C12** alkyl chains, and provides insight into monolayer coverage. Figure 3.2 shows the high-resolution spectra of the C 1s orbital, observed for samples produced by submerged microcontact printing in water. The figure is inlaid with five spectra; the as-received germanium sample (red trace), the 1:1 water/ethanol rinsed bare germanium sample (green trace), full coverage SAM on germanium (purple trace), no-ink stamp sample (control, blue trace), and microcontact sample (black trace).

Previously addressed in chapter 2 was the adventitious adsorption of carbon by the native oxide layer. Again, we see a significant carbon signature for the as-received sample. After rinsing, the oxide is removed, along with its adsorbed carbon, explaining the strong decrease in peak intensity for the bare germanium sample. The SAM sample shows the highest intensity of any peak, evident of its high-coverage monolayer. The SμCP sample exhibits a peak approximately one-half the intensity of the fully formed monolayer and positioned at an identical energy value. The correspondence to the **C12** sample, in terms of location, indicates similarity between carbon atoms, suggesting the presence of a partial monolayer. The lower peak intensity shows that the monolayer achieved only 50% coverage. A control sample, patterned with an un-inked PDMS stamp, confirms that the inking solution was the sole source of carbon deposition. The control sample shows a minimal peak, suggesting limited influence on deposition.

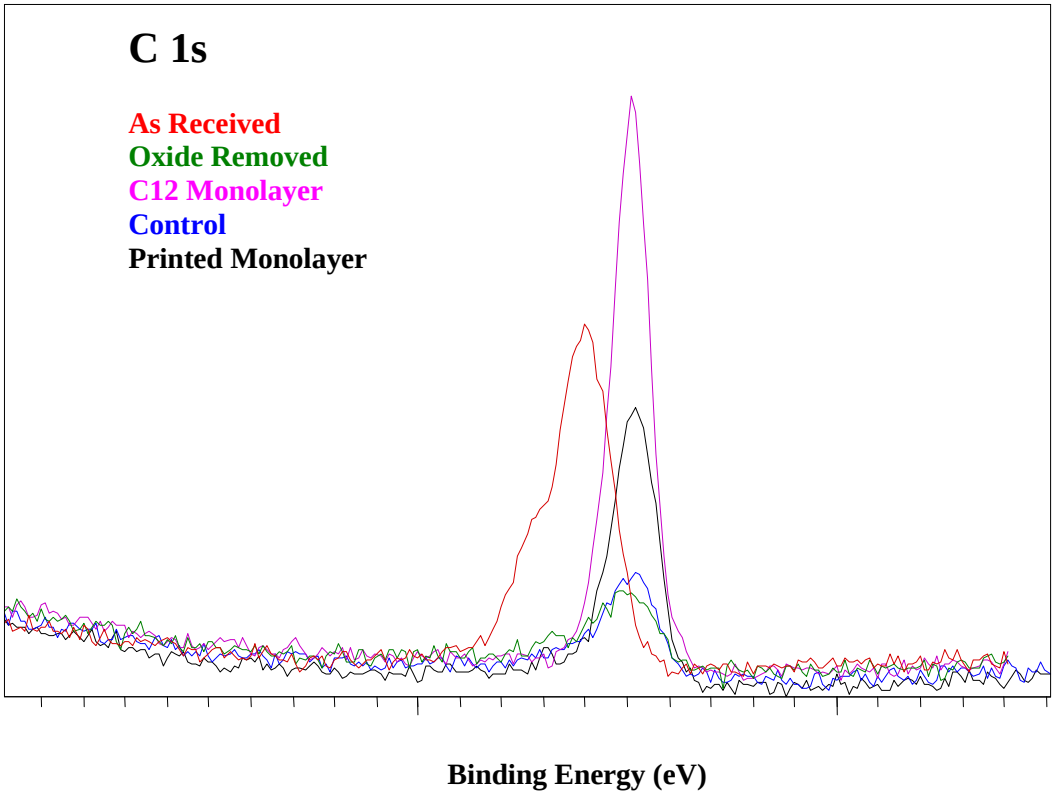

Figure 3.2: High-resolution XPS spectra collected for the region specific to the C 1s orbital. The adventitious carbon of the as-received sample (red trace), is effectively removed by rinsing with water/ethanol (green trace), allowing a high-quality **C12** monolayer (purple trace) to form. Our method for submerged microcontact printing on germanium produces a monolayer of 50% coverage (black trace).[64]

In an attempt to improve monolayer coverage, the sample was submerged in HCl for SμCP. Attempting to chlorinate the surface did not improve the SAM coverage.

3.4.3 Scanning Electron Microscopy Analysis

Scanning electron microscopy images were used to analyze patterned germanium. Figure 3.3 shows a FESEM image of a **C12**-patterned germanium substrate. The SEM images show square patterns exhibiting crisp, clean edge fidelity, indicative of a nearly perfect transfer of stamp features.

Despite the excellent pattern transfer, features were still at submonolayer coverage. Backfilling stamped samples with **MUDA** was performed to heal empty locations, both inside and outside regions of stamp contact, and thus to protect the integrity of the sample surface. The resulting SEM image, shown in Figure 3.4, showed low-intensity squares on a higher intensity background (an inversion of Figure 3.3). The inversion of pattern color suggests **MUDA** monolayer formation.[50] The moderate contrast between patterned and filled locations results from the low surface coverage of the patterned SAMs. Through backfilling, we showed the ability to control the chemistry both inside and outside of the square pattern features. Furthermore, the retained pattern fidelity is indicative of **C12** monolayer stability, and the gentle and non-damaging nature of the backfilling method.

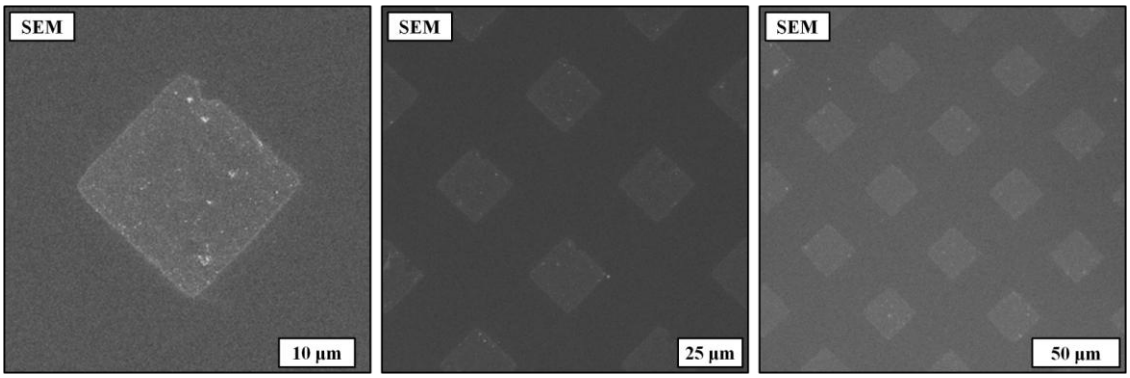

Figure 3.3: Scanning electron microscopy images of **C12** monolayers, patterned on germanium (100). Images represent a single patterned surface at varying resolutions.[64]

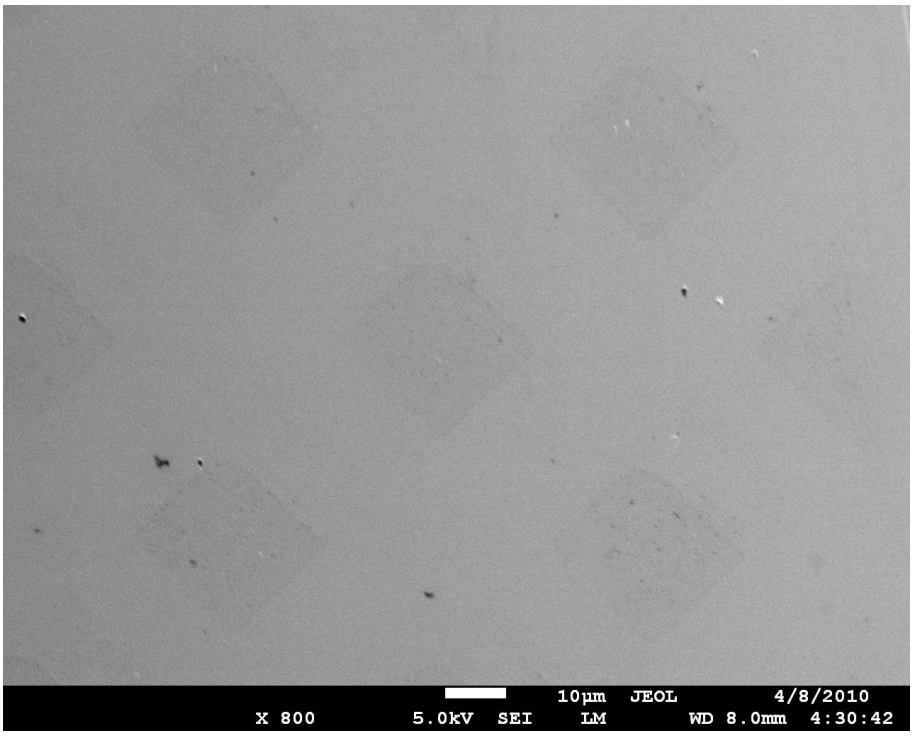

Figure 3.4: Scanning electron microscopy image of a **C12** monolayer, patterned on germanium (100), backfilled with **MUDA**. The inversion of intensity, in comparison with the untreated **C12** monolayer, is indicative of **MUDA** SAM formation. Successful backfilling represents our ability to control the chemistry of both the patterned and non-patterned regions. Retained edge fidelity of the patterned squares shows the non-damaging nature of the backfilling procedure and the stability of the monolayers. A lack of **C12** monolayer coverage results in limited contrast between regions.[64]

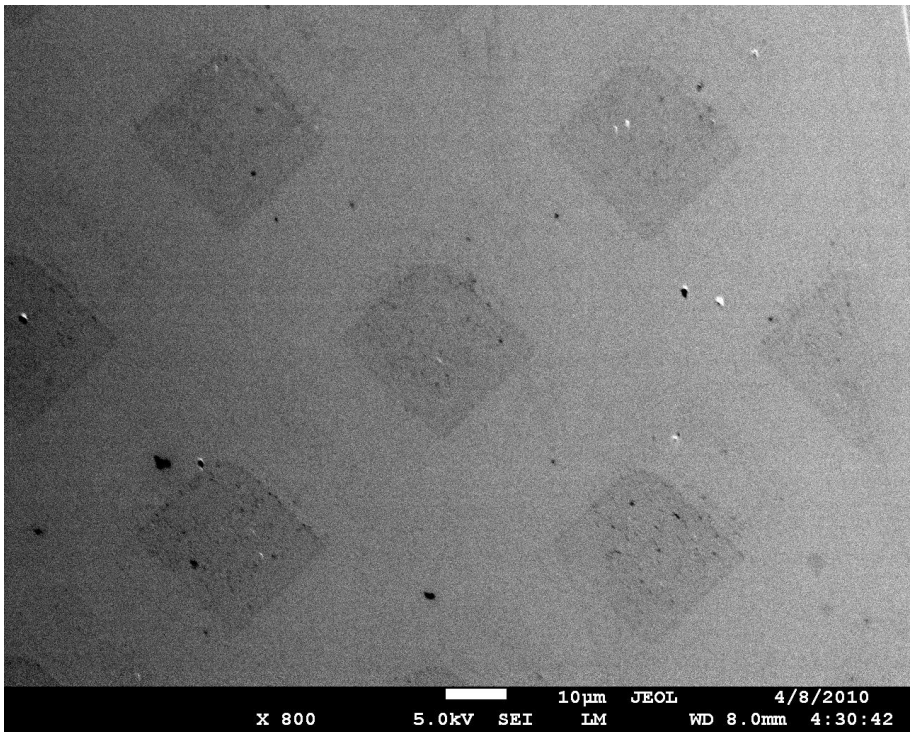

Figure 3.5: Scanning electron microscopy image of a **C12** monolayer, patterned on germanium (100), backfilled with **MUDA**. This image is a contrast enhanced version of Figure 3.4, so as to simplify feature decipherability. The inversion of intensity, in comparison with the untreated **C12** monolayer, is indicative of **MUDA** SAM formation. Successful backfilling represents our ability to control the chemistry of both the patterned and non-patterned regions. Retained edge fidelity of the patterned squares shows the non-damaging nature of the backfilling procedure and the stability of the monolayers. A lack of **C12** monolayer coverage results in limited contrast between regions.[64]

3.5 Conclusions

We have successfully demonstrated the ability to pattern alkanethiol monolayers on Ge(100) through utilization of submerged microcontact printing. Transferring patterns at 100% coverage remains a priority. Further investigation is required to identify the factors inhibiting coverage. Re-oxidation of the germanium surface has been suggested as one possible cause for a lack in coverage. The failure to produce films on bare germanium is consistent with this hypothesis, as the substrate is not protected from oxygen. In SμCP, re-oxidation may occur as water is expelled at contact sites, and thus can no longer remove oxide in these areas. Upon contact, the stamp may displace the water medium, allowing contact between surface and oxygen. This was expected to have been resolved by the passivating ability of HCl, but no improvements in coverage were observed. Preliminary work has indicated that a correlation between stamp and surface wettability may improve results. With continued work, we hope to produce patterned assemblies comparable in order, coverage and functionality, to both those of thiols on gold, and the ones we deposited on germanium.

Chapter 4

Conclusions and Future Prospects

4.1 Review

Techniques for self-assembly and chemical patterning are largely oriented toward the deposition of alkanethiols on gold substrates because of the well-ordered, stable, and chemically functional monolayers produced at the thiol/Au interface. The ability to deposit and to pattern stable thin-films on semiconductor substrates is increasingly relevant. This dissertation has focused on new methods for applying self-assembly and patterning techniques to germanium.

Chapter 2 discussed our development of a one-pot synthesis technique for self-assembly on germanium. Previous studies explained multi-step processes for the removal of germanium's native oxide layer, passivation of its surface by chemical etching, and solution deposition of alkanethiol monolayers. By controlling deposition conditions, we were able to remove the oxide and deposit the SAM simultaneously, in a single step, simplifying the process. We were able to show conclusively that oxide removal, and not surface passivation, is the critical factor for self-assembly on germanium. In Chapter 3, we described the ability to apply soft lithography techniques to patterning germanium substrates. Incomplete monolayer coverage remains a challenge, presumably a result of surface re-oxidation before the monolayer has time to form.

Improving these techniques, and applying these methods, will simplify self-assembly on germanium such that it will become a technologically relevant technique for controlling germanium interfacial chemistry.

4.2 Future Work

Self-assembly on germanium is in its earliest stages, with significant work remaining to develop germanium's full range of capabilities. First, the inhibiting factors in SAM formation must be identified, the sources of which must be addressed. Next, new techniques must be incorporated both to characterize and to improve upon monolayer formation.

Re-oxidation of the surface has been proposed as an important factor that both limits SAM formation, and is responsible for the degradation of formed monolayers.[6] X-ray photoelectron spectroscopy analysis confirms the presence of oxygen on samples containing SAMs. We suggest that defect sites in the SAM allow oxygen to interact with the germanium surface, allowing re-oxidation to occur. It is difficult to produce an entirely defect-free monolayer, so monolayers of germanium will always be susceptible to degradation. We propose that instead of using the thiolate monolayer as a passivating agent, it could instead be used to functionalize the surface for application of high-performance dielectric films, which would, in turn, prevent formation of germanium's oxide layer. It has already been established that alkanethiols exhibit the ability to form monolayers on germanium.[6, 25, 87, 88] They are also capable of being terminated with numerous functional groups.[12] If patterning methods improve to incorporate hybrid techniques, such as microcontact insertion printing, control over the placement and type of the adsorbate layers could potentially aid in the stability of the monolayer and its ability to accept thin films, subsequently making it device-ready. The success of such a strategy is reliant upon the ability to produce full-coverage and stable monolayers *via* numerous chemical patterning techniques, a large library of molecules for

self-assembly, and the ability to characterize and to further manipulate the electronic properties of the resulting sample. To accomplish this, it will be necessary to tweak and to test new combinations of adsorbates, solvents, crystalline planes, insertion methods, and analysis equipment.

4.2.1 Chemicals, Solvents, and Crystalline Planes

The ultimate motivation for studying monolayer deposition on germanium is the potential for a new, faster, generation of electronic devices. It is necessary to establish a reproducible and cost-effective method for device fabrication, so simple, cheap, and atmospherically insensitive procedures and devices are required. Continued tinkering with variable substrate and adsorbate combinations may enable production of such apparatus.

Variations in chemical adsorbates, solvents, and crystalline planes have exhibited the ability to alter sample quality. Wang and co-workers showed that the stability of germanium nanowires increased linearly with alkyl chain length.[89] They attributed the increase in stability to stronger inter-chain van der Waals interactions, and superior density of molecular films, a common characteristic of longer carbon chains. Greater film density affords better oxygen blocking ability. Depositing **C12** monolayers on germanium nanowires produced a sample capable of resisting re-oxidation for 24 hours of ambient exposure.[89] Alkyl chains longer than **C12** were not studied. If further analyses show results consistent with those of **C2**-**C12**, a new standard for surface passivation may be developed. We completed preliminary work that suggests a decrease in solubility as a function of increase in chain length, where **C18** failed to dissolve in solutions adequate

for **C12**. Novel chemistries will be required to solve this and similar problems. It is well known that the ability of alkanethiols to dissolve in solution is dependent upon the type of solvent. As a result, methanol exhibits an enhanced ability, compared to ethanol and *t*-butanol, to enable SAM formation on germanium at both high- and low-water concentration mixtures. This leads us to conclude that any adsorbate may be deposited if optimal solution conditions are met.

The germanium crystallographic orientation can have a large effect on SAM quality. Ardalan and co-workers showed superior monolayer quality on Ge(100), compared to that on Ge(111).[6] Determining the structure of the monolayer on each face will enable us to design better assemblies on germanium surfaces. Other variables have not been ruled out as possible factors in film quality. Further investigation is required to determine the optimal conditions for SAM formation.

4.2.2 Extending Chemical Patterning

Incomplete monolayer coverage remains a challenge, the source of which must be identified and addressed. Ultimately, we would like to extend other patterning techniques to germanium to enhance adsorbate placement and chemical functionality. We believe that extending characterization of soft lithography techniques will lead directly to the development of more precise and efficient methods for technological applications. Both microcontact insertion printing and microdisplacement printing are powerful techniques for their abilities to increase molecular placement selectivity, to limit feature diffusion, and to prepare multi-functional surfaces composed of numerous exposed functionalities. Extending techniques comparable to those applied for chemical patterning on gold will

produce results similar to our work in microcontact printing. Careful analysis and the development of new chemistry techniques will have a significant impact on future soft lithography of many materials.

4.2.3 Infrared Reflection Absorption Spectroscopy (IRRAS)

Infrared reflection absorption spectroscopy is one of the most efficient tools for characterizing the bonding and chemical interactions of molecules on surfaces. It is an important tool for evaluating interface properties, structures, monolayer stability, and functional group identification. This spectroscopic technique introduces infrared radiation to the substrate surface at a grazing angle, exciting vibrational modes of surface species, and reflecting from the surface to a detector. Adsorbed species absorb energy from the incident radiation, proportional to that of vibrational modes. Vibrations correspond to stretching modes induced by slightly differing energies as shown in Figure 4.1. As in XPS, the surface species exhibit unique vibrational frequencies, thus, detected radiation can identify the surface components.

We have utilized IRRAS for characterizing self-assembled monolayers on gold. Figure 4.2 shows a typical IR spectra for **C12** SAMs on Au{111}. This proved to be an excellent diagnostic for analyzing the kinetic behavior of self-assembly on Au{111}. Unfortunately, germanium's transparency to and reflection of infrared radiation precludes its facile use with grazing angle IRRAS experiments. To study monolayer properties, adsorbate-substrate binding mechanisms, and functional groups on alkyl chains, we must alter our techniques for Ge SAM analyses.

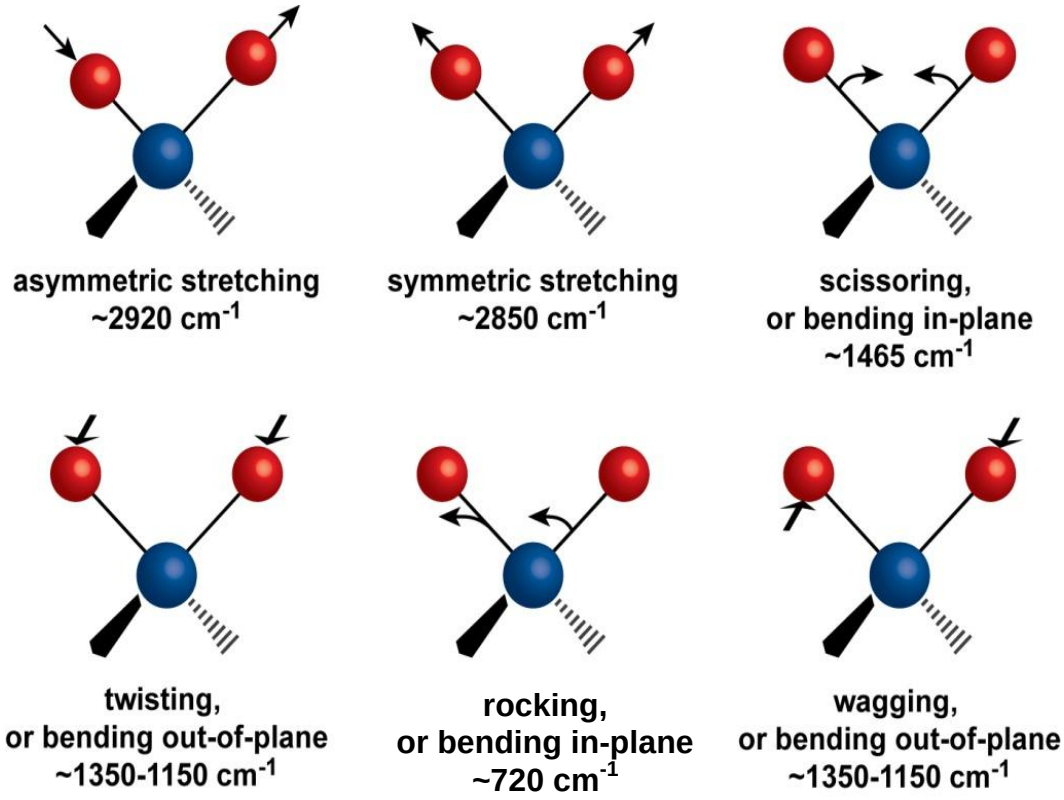

Figure 4.1: Stretching and bending vibrational modes of methylene *(–CH_2–)* groups.[38]

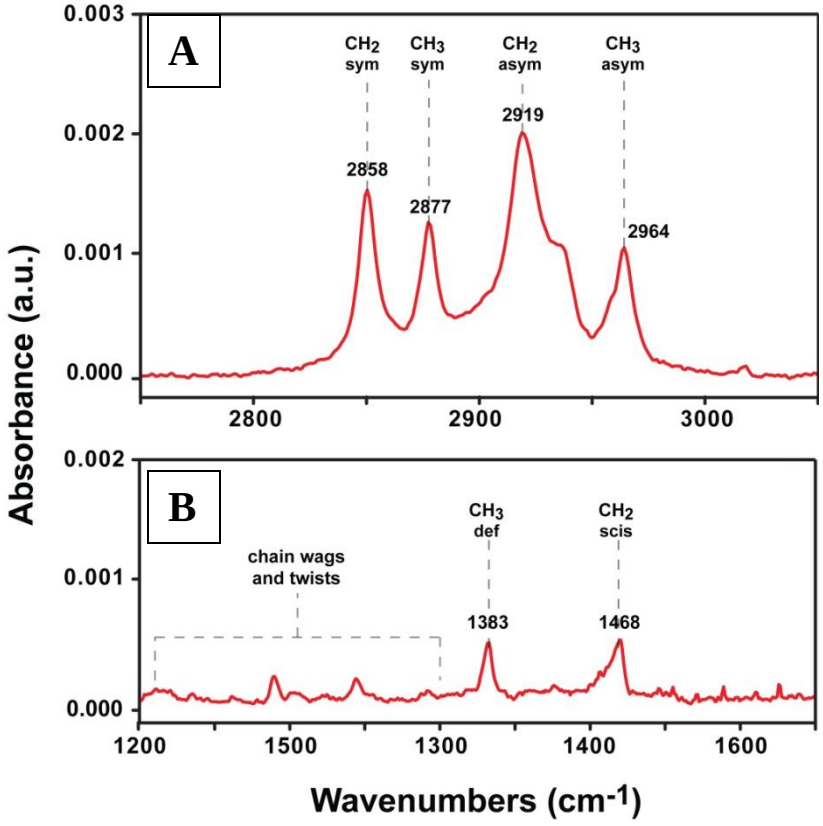

Figure 4.2: Infrared reflection absorption spectroscopy spectra of a **C12** SAM on Au{111}, showing higher energy stretching modes **(A)**, and lower energy bending and wagging modes **(B)**.[38]

Infrared radiation at near-normal incidence to a highly reflective metallic surface will result in a standing wave, resultant from the interaction between incident and reflected wave. The electric-field produced from the standing wave will exhibit an amplitude of zero at the surface, inhibiting interaction between the surface and any adsorbed layers, making obtainment of surface molecule spectra impossible.[107] Monolayers of an array of adsorbates, including thiols, CO, and H_2SO_4, on metallic surfaces, including platinum, gold, and various semiconductors, to name a few, have been analyzed by IRRAS equipment configured with an attenuated-total-reflectance (ATR) configuration.[108-112] Attenuated-total-reflectance surface-enhanced infrared reflection absorption spectroscopy (ATR-SEIRRAS), offers strong signal sensitivity and negligible interference from bulk materials.[113, 114] Attenuated-total-reflectance SEIRRAS measurements have exhibited the ability to produce strong absorption spectra for samples closely related to germanium; monolayers on silicon.[108, 109] In ATR applications, a medium of high refractive index is optically contacted with a medium of low refractive index (an adsorbing medium).[115] The high refractive medium acts as an internal reflection element (IRE) and is transparent to infrared radiation. Incident infrared radiation impinges upon the IRE and passes into the absorbing medium-IRE interface with an angle of incidence greater than the critical angle. In the absence of an absorbing medium, the light will be totally reflected at the interface.[115] In the presence of an absorbing medium, some reflection intensity will be lost in the form of evanescent waves. Figures 4.3 and 4.4 show a schematic of the ATR assembly and a depiction of the evanescent wave, respectively. Evanescent wave formation is explained by the Schrödinger wave function, which states that the electric and magnetic fields cannot be

discontinuous at a boundary. In our case, the absorbing medium is a thiol monolayer, and the IRE is the germanium substrate. Upon reflection at the boundary, a loss in incident beam energy, proportional to the vibrational properties of the interface, occurs in the form of evanescent wave formation.[115] As a result, the collection of absorption spectra becomes possible. The number of reflections is dependent upon material properties and experimental values, such as angle of incidence, and incident beam polarization.[115] The nature of ATR produces a strong IR signal representative of the surface species and not the substrate material. Therefore, it is a powerful technique for observing monolayer properties on germanium.

4.3 Conclusions and Final Thoughts

The electronics industry is making a rapid transition toward a new generation of fast, and highly diverse devices. Fabrication of such components requires materials exhibiting both superior electronic characteristics, and the capability to perform at the nanoscale. Germanium has excellent intrinsic electrical properties, and control of its interfacial chemistry by self-assembly is powerful. Furthermore, it lends itself to a number of modern applications. Complications involving its oxide layer, resulting in instability and deposition difficulties, are currently being studied.

We have begun to address the issues of self-assembly on germanium. This dissertation demonstrated that self-assembly and μCP can be applied to the Ge(100) surface. Several factors inhibit SAM quality and we have gained some insight into the solutions to these problems. Further analyses will improve upon this work and assist in

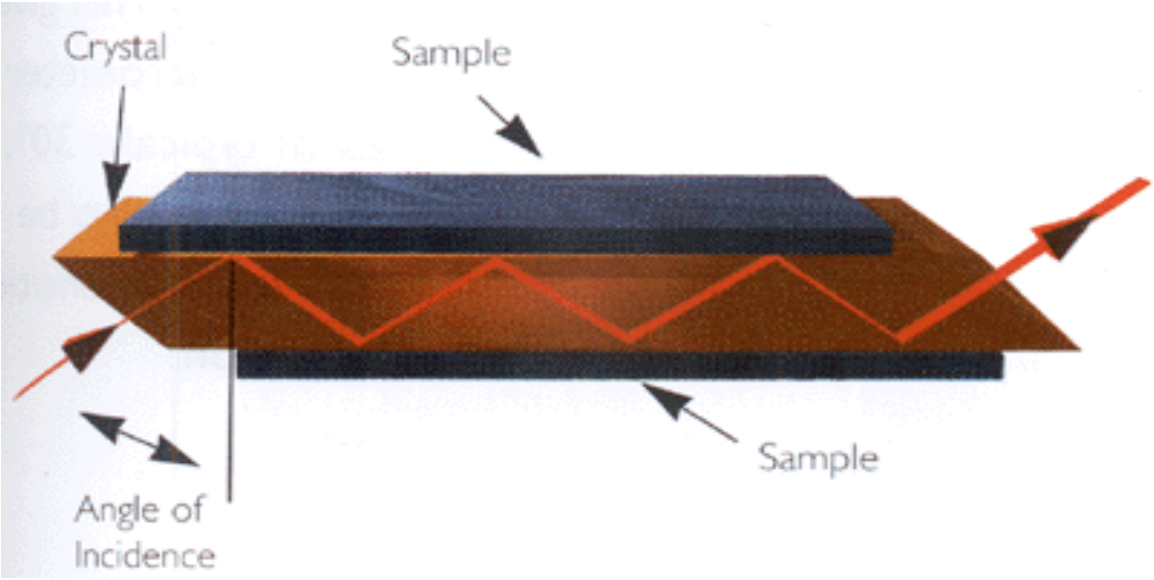

Figure 4.3: Schematic of the attenuated total reflectance assembly. An absorbing medium is placed in intimate contact with an infrared transparent crystal, the internal reflection element. The angle of incidence is set such that it exceeds the critical angle, ensuring total internal reflection. The crystal edges are cut as to allow entrance and emission of incident beam radiation.[116]

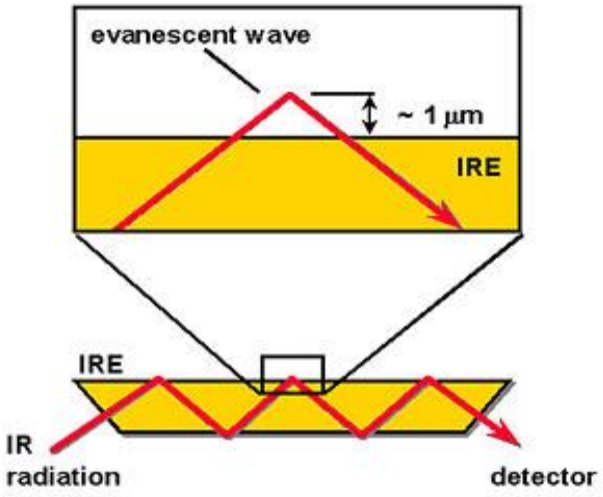

Figure 4.4: Schematic depicting the formation of an evanescent wave as a result of total internal reflection. Upon contact with the IRE boundary, an electric field, in the form of an evanescent wave will develop, as described by Schrödinger's wave function. In the presence of an absorbing medium, the incident beam will experience a reduction in intensity, corresponding to the medium's absorption of the evanescent wave, making absorption spectra collection possible.[117]

the development of industry-ready techniques for SAMs on technological surfaces. Eventually, the investigation of germanium's capacity to interact with technologically important materials may yield the stable, electronically-advanced device, required for the next generations of electronics.

Appendix 1

Non-Technical Abstract

A.1 Non-Technical Abstract

The focus on faster, smaller, and more diverse electronic devices has prompted research into new materials. The search is on for semiconductor substrates with superior electronic capabilities. Germanium has emerged as a semiconductor material capable of producing the performance required for semiconductor devices, but has materials properties that have limited its application. Methods for improving the stability and performance of electronic materials have been developed. In order to manufacture electronic components, both designed from new materials and capable of integration into existing devices, established methods for material manipulation must be adapted. This dissertation will address the issues connected to extending established techniques to new materials, particularly germanium. It is our hope that studying both the ability and limitations of these techniques will lead to the development of industrially relevant procedures and devices.

Germanium's surface is characterized by instability. The chemical make-up of germanium's surface inhibits its ability to interact with materials necessary for device fabrication, thus limiting its capacity for integration. Self-assembled monolayers (SAMs) are the result of molecular adsorption on solid surfaces. The organization and chemical characteristics of SAMs allow them to form on, to stabilize, and to control the properties of a number of substrates. Successful deposition of SAMs on germanium can correct its intrinsic limitations. This dissertation investigates techniques capable of achieving SAM deposition. Additionally, it will examine procedures exhibiting the capacity to enhance

control of electrical properties as well as the ability to incorporate a broad spectrum of relevant materials. In a process akin to stamping ink designs on paper, chemical patterning deposits adsorbates onto the germanium surface in a formation representing that of a patterned soft polymer stamp. This paper will identify successful techniques for improving the limitations of germanium, identify additional shortcomings, and propose solutions to some of the present problems.

References

(1) Mantooth, B. A.; Weiss, P. S. *Proceedings of the IEEE* **2003**, *91*, 1785-1802.

(2) Mullen, T. J.; Srinivasan, C.; Hohman, J. N.; Gillmor, S. D.; Shuster, M. J.; Horn, M. W.; Andrews, A. M.; Weiss, P. S. *Applied Physics Letters* **2007**, *90*, 063114.

(3) Smith, R. K.; Lewis, P. A.; Weiss, P. S. *Progress in Surface Science* **2004**, *75*, 1-68.

(4) Tirrell, M.; Kokkoli, E.; Biesalski, M. *Surface Science* **2002**, *500*, 61-83.

(5) Kasemo, B. *Surface Science* **2002**, *500*, 656-677.

(6) Ardalan, P.; Musgrave, C. B.; Bent, S. F. *Langmuir* **2009**, *25*, 2013-2025.

(7) Loscutoff, P. W.; Bent, S. F. *Annual Review of Physical Chemistry* **2006**, *57*, 467-495.

(8) Misra, D.; Garg, R.; Srinivasan, P.; Rahim, N.; Chowdury, N. A. *Materials Science in Semiconductor Processing* **2006**, *9*, 741-748.

(9) Moore, G. E. *Electronics* **1965**, *38*, 114-117.

(10) Kittel, C. *Introduction to Solid State Physics*, 7th ed.; John Wiley & Sons, Inc.: New York, 1996.

(11) Adamson, A. W.; Gast, A. P. *Physical Chemistry at Surfaces*, 6th ed.; Wiley-Interscience: New York, 1997.

(12) Love, J. C.; Estroff, L. A.; Kriebel, J. K.; Nuzzo, R. G.; Whitesides, G. M. *Chemical Reviews.* **2005**, *105*, 1103-1169.

(13) Kramer, S.; Fuierer, R. R.; Gorman, C. B. *Chemical Reviews* **2003**, *103*, 4367-4418.

(14) Allara, D. L.; Nuzzo, R. G. *Langmuir* **1985**, *1*, 52-66.

(15) Nuzzo, R. G.; Allara, D. L. *Journal of the American Chemical Society* **1983**, *105*, 4481-4483.

(16) Dubois, L. H.; Nuzzo, R. G. *Annual Review of Physical Chemistry* **1992**, *43*, 437-463.

(17) Poirier, G. E. *Chemical Reviews* **1997**, *97*, 1117-1127.

(18) Poirier, G. E.; Tarlov, M. J. *Langmuir* **1994**, *10*, 2853-2857.

(19) Ulman, A. *Chem. Rev.* **1996**, *96*, 1533-1554.

(20) Nuzzo, R. G.; Zegarski, B. R.; Dubois, L. H. *Journal of the American Chemical Society* **1987**, *109*, 733-740.

(21) Ulman, A.; Eilers, J. E.; Tillman, N. *Langmuir* **1989**, *5*, 1147-1152.

(22) Stranick, S. J.; Atre, S. V.; Parikh, A. N. *Nanotechnology* **1996**, *7*, 438-442.

(23) Stranick, S. J.; Parikh, A. N.; Tao, Y. T. *Journal of Physical Chemistry B* **1994**, *98*, 7636-7646.

(24) Yan, L.; Huck, W. T. S.; Whitesides, G. M. *Journal of Macromolecular Science-Polymer Reviews* **2004**, *C44*, 175-206.

(25) Hohman, J. N.; Kim, M.; Lawrence, J. A.; McClanahan, P. D.; Weiss, P. S. *In. Prep. Journal of the American Chemical Society* **2010**.

(26) Bent, S. F. *ACS Nano* **2007**, *1*, 10-12.

(27) Bermudez, V. M. *Langmuir* **2003**, *19*, 6813-6819.

(28) Zerulla, D.; Chasse, T. J. *Electronics Spectroscopy* **2009**, *172*, 78-87.

(29) Wolpers, M.; Viefhaus, H.; Stratman, M. *Applied Surface Science* **1990**, *45*, 167-170.

(30) Cimatu, K.; Baldelli, S. *Journal of Physical Chemistry C* **2007**, *111*, 7137-7143.

(31) Love, J. C.; Wolfe, D. B.; Chabinyc, M. L.; Paul, K. E.; Whitesides, G. M. *Journal of the American Chemical Society* **2002**, *124*, 1576-1577.

(32) Schlenoff, J. B.; Li, M.; Ly, H. J. *Journal of the American Chemical Society* **1995**, *117*, 12528-12536.

(33) Poirier, G. E.; Pylant, E. D. *Science* **1996**, *272*, 1145-1149.

(34) Laibinis, P. E.; Whitesides, G. M.; Allara, D. L. *Journal of the American Chemical Society* **1991**, *113*, 7152-7167.

(35) Schreiber, F. *Progress in Surface Science* **2000**, *65*, 151-256.

(36) Nishi, N.; Hobara, D.; Yamamoto, M.; Kakiuchi, T. *Journal of Chemical Physics* **2003**, *118*, 1904-1911.

(37) Yang, G. H.; Liu, G. Y. *Journal of Physical Chemistry B* **2003**, *107*, 8746-9759.

(38) Saavedra, H. M. Ph.D. Thesis, The Pennsylvania State University, University Park, PA, USA, 2010.

(39) Cassie, A. B. D.; Baxter, S. *Transactions of the Faraday Society* **1944**, *40*, 546-551.

(40) Li, D.; Neumann, A. W. In *Applied Surface Thermodynamics*; Spelt, J. K., Ed.; Marcel Dekker, Inc.: New York, 1996; Vol. 63, pp 109-168.

(41) Kwok, D. Y.; Gietzelt, T.; Grundke, K.; Jacobasch, H. J.; Neumann, A. W. *Langmuir* **1997**, *13*, 2880-2894.

(42) Gennes, P. G. d.; Brochard-Wyart, F.; Quere, D. *Capillarity and Wetting Phenomena: Drops, Bubbles, Pearls, Waves*; Springer Verlag: New York, 2004.

(43) MacRitchie, F. *Chemistry at Interfaces*; Academic Press, Inc.: San Diego, 1990.

(44) Kolasinski, K. W. *Surface Science: Foundations of Catalysis and Nanoscience*; John Wiley & Sons, Inc.: Wes Sussex, 2002.

(45) Gaydos, J.; Neumann, A. W. In *Applied Surface Thermodynamics*; Spelt, J. K., Ed.; Marcel Dekker, Inc.: New York, 1996; Vol. 63, pp 169-238.

(46) Wenzel, R. N. *Industrial and Engineering Chemistry* **1936**, *28*, 988-994.

(47) McClanahan, P. D. Honors, Pennsylvania State University, State College, 2009.

(48) Spelt, J. K.; Vargha-Butler, E. I. In *Applied Surface Thermodynamics*; Spelt, J. K., Ed.; Marcel Dekker, Inc.: New York, 1996; Vol. 63, pp 379-411.

(49) Lander, L. M.; Siewierski, L. M.; Brittain, W. J.; Vogler, E. A. *Langmuir* **1993**, *9*, 2237-2239.

(50) Srinivasan, C.; Mullen, T. J.; Hohman, J. N.; Anderson, M. E.; Dameron, A. A.; Andrews, A. M.; Dickey, E. C.; Horn, M. W.; Weiss, P. S. *ACS Nano* **2007**, *1*, 191-201.

(51) Qin, D.; Xia, Y. N.; Whitesides, G. M. *Nature Proocols* **2010**, *5*, 491-502.

(52) Xia, N.; Thodeti, C. K.; Hunt, T. P.; Xu, Q. B.; Ho, M.; Whitesides, G. M.; Westervelt, R.; Ingber, D. E. *Faseb Journal* **2008**, *22*, 1649-1659.

(53) Wang, Y.; Mirkin, C. A.; Park, S. J. *ACS Nano* **2009**, *3*, 1049-1056.

(54) Saavedra, H. M.; Mullen, T. J.; Zhang, P.; Dewey, D. C.; Claridge, S. A.; Weiss, P. S. *Reports on Progress in Physics* **2010**, *73*, 1-40.

(55) Delamarche, E.; Schmid, H.; Bietsch, A.; Larsen, N. B.; Rothuizen, H.; Michel, B.; Biebuyck, H. *Journal of Physical Chemistry B* **1998**, *102*, 3324-3334.

(56) Libioulle, L.; Bietsch, A.; Schmid, H.; Michel, B.; Delamarche, E. *Langmuir* **1999**, *15*, 300-304.

(57) Larsen, N. B.; Biebuyck, H.; Delamarche, E.; Michel, B. *Journal of the American Chemical Society* **1997**, *119*, 3017-3026.

(58) Wilbur, J. L.; Kumar, A.; Kim, E.; Whitesides, G. M. *Advanced Materials* **1994**, *6*, 600-604.

(59) Dameron, A. A.; Hampton, J. R.; Smith, R. K.; Mullen, T. J.; Gillmor, S. D.; Weiss, P. S. *Nano Letters* **2005**, *5*, 1834-1837.

(60) Moulder, J. F.; Stickle, W. F.; Sobol, P. E.; Bomben, K. D. *Handbook of X-ray Photoelectron Spectroscopy*; Perkin-Elmer Corporation: Eden Prairie, 1992.

(61) Prabhakaran, K.; Maeda, F.; Watanabe, Y.; Ogino, T. *Applied Physics Letters* **2000**, *76*, 2244-2246.

(62) Rivillon, S.; Chabal, Y. J. *Applied Physics Letters* **2005**, *87*, 253101-253103.

(63) Prabhakaran, K.; Ogino, T. *Surface Science* **1995**, *325*, 263-271.

(64) Hohman, J. N.; Lawrence, J. A.; Weiss, P. S. *Unpublished Results* **2010**.

(65) Han, S. M.; Ashurst, W. R.; Carraro, C.; Maboudian, R. *Journal of the American Chemical Society* **2001**, *123*, 2422-2425.

(66) He, J.; Lu, Z.-H.; Mitchell, S. A.; Wayner, D. D. M. *Journal of the American Chemical Society* **1998**, *120*, 2660-2661.

(67) Kosuri, M. R.; Cone, R.; Li, Q.; Han, S. M. *Langmuir* **2004**, *20*, 835-840.

(68) Cullen, G. W.; Amick, J. A.; Gerlich, D. *Journal of the Electrochemical Society* **1962**, *109*, 124-127.

(69) Lu, Z. H. *Applied Physics Letters* **1996**, *68*, 520-522.

(70) Roche, J.; Ryan, P.; Hughes, G. J. *Applied Surface Science* **2001**, *174*, 271-274.

(71) Gothelid, M.; LeLay, G.; Wigren, C.; Bjorkqvist, M.; Rad, M.; Karlsson, U. O. *Applied Surface Science* **1997**, *115*, 87-95.

(72) Weser, T.; Bogen, A.; Konrad, B.; Schnell, R. D.; Schug, C. A.; Steinmann, W. *Physical Review B* **1987**, *35*, 8184-8188.

(73) Kosuri, M. R.; Cone, R.; Li, Q.; Han, S. M. *Langmuir* **2004**, *20*, 835-840.

(74) Shirley, D. A. *Physical Review B* **1972**, *5*, 4709-4714.

(75) Bain, C. D.; Troughton, E. B.; Tao, Y. T.; Evall, J.; Whitesides, G. M.; Nuzzo, R. G. *Journal of the American Chemical Society* **1989**, *111*, 321-335.

(76) Bain, C. D.; Whitesides, G. M. *Science* **1988**, *240*, 62-63.

(77) Nuzzo, R. G.; Dubois, L. H.; Allara, D. L. *Journal of the American Chemical Society* **1990**, *112*, 558-569.

(78) Laibinis, P. E.; Bain, C. D.; Whitesides, G. M. *Journal of Physical Chemistry* **1991**, *95*, 7017-7021.

(79) Folkers, J. P.; Laibinis, P. E.; Whitesides, G. M. *Langmuir* **1992**, *8*, 1330-1341.

(80) Biebuyck, H. A.; Bian, C. D.; Whitesides, G. M. *Langmuir* **1994**, *10*, 1825-1831.

(81) Tabet, N.; Faiz, M.; Hamdan, N. M. *Surface Science* **2003**, *523*, 68-72.

(82) Hanrath, T.; Korgel, B. A. *Journal of the American Chemical Society* **2004**, *126*, 15466-15472.

(83) Porter, L. A.; Choi, H. C.; Ribbe, A. E.; Buriak, J. M. *Nano Letters* **2002**, *2*, 1067-1071.

(84) Wojtyk, J. T. C.; Tomietto, M.; Boukherroub, R.; Wayner, D. D. M. *Journal of the American Chemical Society* **2001**, *123*, 1535-1536.

(85) Ivanisevic, A.; Mirkin, C. A. *Journal of the American Chemical Society* **2001**, *123*, 7887-7889.

(86) Maynor, B. W.; Filocamo, S. F.; Grinstaff, M. W.; Liu, J. *Journal of the American Chemical Society* **2001**, *124*, 522-523.

(87) Elshocht, S. V.; Brijs, B.; Caymax, M.; Conard, T.; Chiarella, T.; Gendt, S. D.; Jaeger, B. D.; Kubicek, S.; Meuris, M.; Onsia, B.; Richard, O.; Teerlinck, I.; Steenbergen, J. V.; Zhao, C.; Heyns, M. *Applied Physics Letters* **2004**, *85*, 3824-3826.

(88) Wang, D.; Dai, H. *Applied Physics A* **2006**, *85*, 217-225.

(89) Wang, D.; Chang, Y. L.; Liu, Z.; Dai, H. *Journal of the American Chemical Society* **2005**, *127*, 11871-11875.

(90) Stanley, S. K.; Joshi, S. V.; Banerjee, S. K.; Ekerdt, J. G. *Journal of Vacuum Science and Technology A* **2006**, *24*, 78-83.

(91) King, T. J.; Saraswat, K. C. *Journal of the Electrochemical Society* **1994**, *141*, 2235-2241.

(92) Zanier, S.; Guldner, Y.; Berroir, J. M.; Vieren, J. P.; Faini, G.; Cambril, E.; Garchery, L.; Campidelli, Y.; Sagnes, I. *Thin Solid Films* **1997**, *294*, 315-317.

(93) Okamoto, S.; Maruyama, E.; Terakawa, A.; Shinohara, W.; Nakano, S.; Hishikawa, Y.; Wakisaka, K.; Kiyama, S. *Solar Energy Materials & Solar Cells* **2001**, *66*, 85-94.

(94) Izyumskaya, N.; Alivov, Y.; Morkoc, H. *Critical Reviews in Solid State and Materials Sciences* **2009**, *34*, 89-179.

(95) Monget, C.; Schiltz, A.; Joubert, O.; Vallier, L.; Guillermet, M.; Tormen, B. *Journal of Vacuum Science and Technology B* **1998**, *16*, 1833-1840.

(96) Rao, R.; Bradby, J. E.; Williams, J. S. *Applied Physics Letters* **2007**, *91*, 1231131-1231133.

(97) Tillack, B.; Richter, H. H.; Ritter, G.; Wolff, A.; Morgenstern, G.; Eggs, C. *Journal of Vacuum Science and Technology B* **1996**, *14*, 102-105.

(98) Lopinski, G. P.; Eves, B. J.; Hul'ko, O.; Mark, C.; Patistas, S. N.; Boukherroub, R.; Ward, T. R. *Physical Review B* **2005**, *71*, 1253081-1253084.

(99) Choi, K.; Buriak, J. M. *Langmuir* **2000**, *16*, 7737-7741.

(100) Kim, H.; McIntyre, P. C.; Chui, C. O.; Saraswat, C.; Cho, M. H. *Applied Physics Letters* **2004**, *85*, 2902-2904.

(101) Magagnin, L.; Maboudian, R.; Carraro, C. *Journal of Physical Chemistry B* **2002**, *106*, 401-407.

(102) Mirkin, C. A. *ACS Nano* **2007**, *1*, 79-83.

(103) Su, M.; Liu, X.; Li, S. Y.; Dravid, V. P.; Mirkin, C. A. *Journal of the American Chemical Society* **2002**, *124*, 1560-1561.

(104) Wang, D.; Thomas, S. G.; Wang, K. L.; Xia, Y.; Whitesides, G. M. *Applied Physics Letters* **1997**, *70*, 1593-1595.

(105) Dameron, A. A.; Hampton, J. R.; Gillmor, S. D.; Hohman, J. N.; Weiss, P. S. *Journal of Vacuum Science and Technology B* **2005**, *23*, 2929-2932.

(106) Bessueille, F.; Pla-Roca, M.; Mills, C. A.; Martinez, E.; Samitier, J.; Errachid, A. *Langmuir* **2005**, *21*, 12060-12063.

(107) Greenler, R. G. *Journal of Chemical Physics* **1966**, *44*, 310-315.

(108) Hartstein, A.; Kirtley, J. R.; Tsang, J. C. *Physical Review Letters* **1980**, *45*, 201-204.

(109) Scheres, L.; Giesbers, M.; Zuilhof, H. *Langmuir* **2010**, *26*, 4790-4795.

(110) Nishikawa, Y.; Fujiwara, K.; Ataka, K.; Osawa, M. *Analytical Chemistry* **1993**, *65*, 556-562.

(111) Bjerke, A. E.; Griffiths, P. R.; Theiss, W. *Analytical Chemistry* **1999**, *71*, 1967-1974.

(112) Wandlowski, T.; Ataka, K.; Pronkin, S.; Diesing, D. *Electrochimica Acta* **2004**, *49*, 1233-1247.

(113) Roseler, A.; Korte, E. H. *Fresenius Journal of Analytical Chemistry* **1998**, *362*, 51-57.

(114) Huo, S. J.; Xue, X. K.; Yan, Y. G.; Li, Q. X.; Ma, M.; Cai, W. B.; Xu, Q. J.; Osawa, M. *Journal of Physical Chemistry B* **2006**, *110*, 4162-4169.

(115) Ekgasit, S.; Ishida, H. In *Handbook of Vibrational Spectroscopy*; Griffiths, P. R., Ed.; John Wiley & Sons, Ltd.: New York, 2002; Vol. 2, pp 1508.

(116) *Attenuated Total Reflectance (ATR)*; Pecsa Analytical, 1990.

(117) Martin-Gil, J.; Palacios-Leble, G.; Ramos, P. M.; Martin-Gil, F. J. *Journal of Interdisciplinary Celtic Studies* **2007**, *5*, 63-76.